

Journal Pre-proof

New trends in the development of electrochemical biosensors for the quantification of microRNAs

Michael López Mujica, Pablo A. Gallay, Fabrizio Perrachione, Antonella E. Montemerlo, Luis A. Tamborelli, Virginia Vaschetti, Daiana Reartes, Soledad Bollo, Marcela C. Rodríguez, Pablo D. Dalmaso, María D. Rubianes, Gustavo A. Rivas



PII: S0731-7085(20)31364-9

DOI: <https://doi.org/10.1016/j.jpba.2020.113478>

Reference: PBA 113478

To appear in: *Journal of Pharmaceutical and Biomedical Analysis*

Received Date: 21 June 2020

Revised Date: 13 July 2020

Accepted Date: 14 July 2020

Please cite this article as: Mujica ML, Gallay PA, Perrachione F, Montemerlo AE, Tamborelli LA, Vaschetti V, Reartes D, Bollo S, Rodríguez MC, Dalmaso PD, Rubianes MD, Rivas GA, New trends in the development of electrochemical biosensors for the quantification of microRNAs, *Journal of Pharmaceutical and Biomedical Analysis* (2020), doi: <https://doi.org/10.1016/j.jpba.2020.113478>

This is a PDF file of an article that has undergone enhancements after acceptance, such as the addition of a cover page and metadata, and formatting for readability, but it is not yet the definitive version of record. This version will undergo additional copyediting, typesetting and review before it is published in its final form, but we are providing this version to give early visibility of the article. Please note that, during the production process, errors may be discovered which could affect the content, and all legal disclaimers that apply to the journal pertain.

© 2020 Published by Elsevier.

New trends in the development of electrochemical biosensors for the quantification of microRNAs

Michael López Mujica¹, Pablo A. Gallay¹, Fabrizio Perrachione¹, Antonella E. Montemerlo¹, Luis A. Tamborelli^{1,2}, Virginia Vaschetti^{1,2}, Daiana Reartes¹, Soledad Bollo³, Marcela C. Rodríguez¹, Pablo D. Dalmaso², María D. Rubianes¹, Gustavo A. Rivas^{1, *}

¹INFIQC(CONICET). Departamento de Fisicoquímica, Facultad de Ciencias Químicas, Universidad Nacional de Córdoba. Ciudad Universitaria, 5000-Córdoba. Argentina; ²CIQA-CONICET, Departamento de Ingeniería Química, Facultad Regional Córdoba, Universidad Tecnológica Nacional. Maestro López esq. Cruz Roja Argentina, 5016-Córdoba, Argentina; ³ Advanced Center for Chronic Diseases (ACCDiS). Facultad de Ciencias Químicas y Farmacéuticas, Departamento de Química Farmacológica y Toxicológica, Universidad de Chile. Santiago, Chile.

HIGHLIGHTS

- -Electrochemical biosensors demonstrated to be an excellent analytical tool to quantify miRNAs.
- -Amplification strategies have allowed to obtain ultrasensitive electrochemical miRNA biosensing.

- -Non-amplified biosensors present competitive analytical performance in shorter times.

Abstract

MicroRNAs (miRNAs) are non-coding regulatory RNAs that play an important role in RNA silencing and post-transcriptional gene expression regulation. Since their dysregulation has been associated with Alzheimer disease, cardiovascular diseases and different types of cancer, among others, miRNAs can be used as biomarkers for early diagnosis and prognosis of these diseases. The methods commonly used to quantify miRNAs are, in general, complex, costly, with limited application for point-of-care devices or resource-limited facilities. Electrochemical biosensors, mainly those based on nanomaterials, have emerged as a promising alternative to the conventional miRNA detection methods and have paved the way to the development of sensitive, fast, and low-cost detection systems. This review is focused on the most relevant contributions performed in the field of electrochemical miRNAs biosensors between 2017 and the beginning of 2020. The main contribution of this article is the critical discussion of the different amplification strategies and the comparative analysis between amplified and non-amplified miRNA electrochemical biosensing and between the different amplification schemes. Particular emphasis was given to the importance of the nanostructures, enzymes, labelling molecules, and special sequences of nucleic acids or analogues on the organization of the different bioanalytical platforms, the transduction of the hybridization event and the generation the analytical signals.

1. General considerations about microRNAs

microRNAs (miRNAs) belong to a class of non-coding RNAs of 19-25 nucleotides in length that present an important role in the post-transcriptional regulation of gene expression [1]. They are crucial regulators of cell differentiation, proliferation, apoptosis and immune response [2, 3]. According to miRBase, there are 1917 miRNAs encoding sequences identified in the human genome [1]. The biogenesis of miRNA is a multi-step process that starts within the nucleus through the action of RNA polymerase II that produces primary miRNA transcripts (pri-miRNAs) of different lengths from the non-coding fraction of the genome. The pri-miRNA is cleaved by a microprocessor complex integrated by a RNase III enzyme (Drosha) and a RNA binding protein called DiGeorge syndrome critical region gene 8 (DGCR8/Pasha), producing the precursor or premature miRNA (pre-microRNA) which contains 60–70 nucleotides. Pre-microRNA is then carried into the cytoplasm by exportin-5 (XPO5) and RanGTPase where the endonuclease called Dicer removes the terminal loops, originating the mature double-stranded microRNA (22 nucleotides long). One strand (passenger strand/complementary strand) is destroyed by Argonaute proteins while the other strand (guide strand/mature strand) is associated with RISC (RNA-induced silencing complex). The mature miRNA interacts with 3' untranslated region (UTR) of target mRNA by one of two mechanisms of gene regulation depending on the degree of complementarity between miRNA and mRNA, either degradation of messenger RNA (mRNA) or repression of mRNA translation. An efficient complementarity leads to mRNA degradation, whereas a limited complementarity guides repression of mRNA translation (Figure 1) [1, 4]. While most of the miRNAs are detected in

the cellular microenvironment, some others, called circulating/extracellular miRNAs, can be also detected in the extracellular environment, including several fluids like colostrum; breast milk; cerebrospinal, peritoneal, amniotic, synovial, pleural, follicular and seminal fluids; tears; saliva; bronchial lavage; urine; plasma and serum [4, 5]. Circulating miRNAs are present in exosomes, microvesicles, apoptotic bodies, complexes with Argonaut proteins, and complexes with high-density lipoproteins to be protected from the RNases degradation [5]. miRNAs play a key role in the regulation of processes related to the development of numerous human diseases such as cancer, cardiovascular, immunological, neurodegenerative, and skin diseases [1, 5-11]. Therefore, they can be regarded as minimally invasive disease biomarkers, useful for the diagnosis, prognosis and treatment of different diseases, with special emphasis in cancer [5-11].

At present, miRNA detection techniques mostly rely on conventional nucleic acid detection assays such as the quantitative reverse transcription polymerase chain reaction (qRT-PCR), the gold standard technique; microarrays; Northern blot and RNA-sequencing [12-14]. Despite the excellent analytical performance offered by these techniques, they are complex and expensive and involve long detection processes. Therefore, they are not suitable for resource-limited facilities and decentralized settings, restricting their real-world application. That is the reason why in the last years there has been an increasing interest for developing different biosensing strategies that make possible the highly sensitive and selective quantification of miRNAs [15, 16]. However, their low abundance, short length and high sequence similarity with other family members, have made the development of miRNAs biosensors a major challenge [17]. In this sense,

electrochemical sensors offer many advantages in terms of sensitivity, selectivity, cost, robustness, portability, compatibility with point-of-care (POC) devices, and large-scale production [18-21]. Particularly, the combination of the electrochemical sensing with Nanobiotechnology, has generated a new class of low-cost, robust, reliable, easy-to-use and ultrasensitive tool for diagnostics and prognosis of several diseases [21].

2. Electrochemical miRNAs biosensors

The most recent electrochemical biosensing schemes for miRNAs have been focused on the evaluation of the DNA-RNA or RNA-RNA duplexes formation mainly through the variation of the charge transfer resistance; the changes of the voltammetric, (chrono)amperometric or chronocoulometric response of different redox markers (either small electroactive compounds, inorganic complexes, redox mediators or intercalators), associated with nanomaterials and signaling enzymes. In the last years, the investigation of new amplification schemes has opened new horizons in the design of sensitive miRNAs biosensors. The main goal of these new developments was the generation of alternatives to qRT-PCR since, as it was already mentioned, in spite of its excellent analytical performance, it presents some draw-backs connected with the cost, time, and requirement of trained personal and special equipment. The engineering of different nucleic acid structures has become an interesting tool to increase the sensitivity of miRNA determinations. In this sense, the hybridization chain reaction (HCR), catalyzed hairpin-assembly (CHA) amplification, rolling circle amplification (RCA), strand displacement amplification

(SDA), and the recycling of target nucleic acids using endonucleases, have been the most widely used strategies.

In the following sections we present the most significant contributions performed in the last three years on the field of miRNA electrochemical biosensors, with a critical discussion about the amplification strategy, the bioanalytical platform and the transduction scheme. Table 1 summarizes the most relevant information for the different biosensors discussed in the manuscript.

2. 1. Amplification-based electrochemical miRNAs biosensors

In this section we discuss the characteristics of the most representative miRNAs electrochemical biosensors organized according to the amplification strategy used to quantify the different miRNAs.

2.1.a. Amplification schemes based on the facilitated accumulation of redox markers

One relatively simple, fast and sensitive amplification approach was focused on the electrostatic accumulation of a redox marker at the miRNA adsorbed at the electrode or at the resulting surface heteroduplex capture-DNA/RNA. Islam et al. [22] reported the use of SPCEs modified with graphene oxide(GO)-loaded iron oxide for the quantification of miRNA-21 at fM level, through the adsorption of purified and magnetically separated miRNA at GO, the accumulation of $[\text{Ru}(\text{NH}_3)_6]^{3+}$ (RuHex) at the negatively charged sugar-phosphate backbone of the nucleic acid, and its chronocoulometric detection catalyzed by $[\text{Fe}(\text{CN})_6]^{3/4-}$. Following a similar scheme, Islam et al. [23] presented the sensitive

and selective electrocatalytic detection of miRNA-107 at Au-loaded nanoporous superparamagnetic-iron oxide nanocubes-modified-SPCE through the catalytic reduction of RuHex electrostatically accumulated at the gold-adsorbed miRNA, allowing the sub-fM detection and the successful application for the quantification in cancer cell lines and samples of oesophageal squamous cell carcinoma. Su et al. [24] proposed the detection of sub-fM levels of miRNA-21 based on the use of gold nanoparticles (AuNPs)-decorated MoS₂ nanosheets (AuNPs@MoS) in two-directions, as platform for the immobilization of capture DNA and as signal-amplifier and support for the signaling DNA. The miRNA-21 sandwich hybridization scheme was established between capture DNA-AuNPs@MoS₂ and signaling DNA-AuNPs@MoS₂, and the analytical signal was obtained either, from the voltammetric (Differential Pulse Voltammetry, DPV) reduction current of the preconcentrated RuHex or from the increment in the charge transfer resistance of [Fe(CN)₆]^{3-/4-} (Figure 2). Ganguly et al. [25] reported the sub-fM non-labeled chronocoulometric detection of miRNA-21 through the redox signal of RuHex electrostatically accumulated at the hybrid generated between the thiolated capture DNA immobilized at MoS₂ nanosheets intimately coupled with electrodeposited AuNPs (AuNPs@MoS₂), the target miRNA-21, and the non-labeled signaling DNA.

2.1.b. Amplification schemes based on the use of endonucleases

The use of endonucleases associated with diverse nanostructures, (bio)catalytic processes and transduction schemes, has received great attention for the development of novel amplified miRNAs biosensing platforms. The most widely used endonuclease was the duplex specific nuclease (DSN), a nuclease that

cleaves double stranded DNAs, or DNAs in DNA-RNA duplexes with at least 15 base pairs, although is inactive to cleave single-stranded DNA, RNA or double stranded RNA [26].

One interesting strategy was focused on the use of a thiolated capture DNA-1-modified Au electrode as bioanalytical platform to detect miRNA-29a-3p through the DSN-mediated hydrolysis of the DNA-1 strand at the (DNA-1/miRNA-29a-3p) surface heteroduplex, the cyclic release of miRNA, the generation of more DNA-RNA heteroduplexes, the decrease of the amount of DNA-1 available to hybridize with DNA-2-AuNPs, and the consequent decrease of the amount of RuHex electrostatically associated to the (DNA-1/DNA-2-AuNPs) (Figure 3) [27]. Bo et al. [28] reported an attomolar-level biosensing scheme for the quantification of miRNA-21 based on the use of a thiolated hairpin probe-modified Au electrode as platform to generate a surface heteroduplex in the presence of miRNA-21 that triggers the cyclic cleavage of the DNA strand mediated by DSN, the final hybridization between the remaining surface-DNA with the bridge signaling DNA-AuNPs, and further preconcentration of RuHex, responsible for the chronocoulometric reduction signal (Figure 4). Another biomarker used to quantify miRNA in connection with the use of DSN, was the anticancer drug doxorubicin. Tao et al. [29] described the ultrasensitive quantification of miRNA-let-7d through the use of a double-loop hairpin probe that possesses a capture sequence, an output segment and its complementary fragment immobilized at the electrode, in association with the signaling AuNPs@Dox@S1. In the presence of miRNA-let-7d the surface heteroduplex generated with the capture sequence allows the action of DSN and the released target triggers a recycling amplification, displacing

AuNPs@Dox@S1, and producing a decrease in the voltammetric (square wave voltammetry, SWV) response of doxorubicin. Other DSN-based amplification strategies were focused on the transduction of the hybridization event from the electrochemical detection of the biocatalytic activity of labelling enzymes like horseradish peroxidase (HRP) and alkaline phosphatase (ALP). Figure 5A shows an interesting biosensing scheme for the attomolar detection of miRNA-21 proposed by Zhang H et al. [30] which involves a triple signal amplification associated with the use of a hairpin DNA modified-gold electrode, the action of DSN-assisted target recycling, and the incorporation of a biotinylated signaling DNA/streptavidin-AuNPs to anchor the biotinylated HRP. Figure 5B shows the typical voltammetric profiles of 3,3',5,5'-tetramethylbenzidine (TMB) obtained in the presence of miRNA-21 due to the biocatalytic activity of the HRP incorporated in the multistructure, effect that is more pronounced as the concentration of the biomarker increases due to the higher accumulation of HRP. Figure 5C depicts the corresponding chronoamperograms for the addition of increasing concentration of miRNA-21. Wang J. et al. [31] presented the immobilization of a capture DNA at bMWCNTs@GO nanoribbons@AuNPs-modified GCE, the cyclic DSN-mediated cleavage of the heteroduplex generated in the presence of miRNA, and further association of the streptavidin-ALP conjugate that generates ascorbic acid from ascorbic-acid phosphate and produces the reduction of iodine. The higher the concentration of miRNA, the lower the amount of the biotinylated signaling DNA at the electrode surface and the lower the analytical signal. Miao et al. [32] reported the use of another endonuclease to develop an interesting alternative for the attomolar quantification of a model miRNA. The scheme was based on a star-

trigon structure and endonuclease-mediated signal amplification using a GCE modified with poly(diallyldimethylammonium chloride) (PDDA) and AuNPs to anchor the MB-labeled-capture probe. Since the capture and auxiliary probes were partially complementary to the miRNA, a star-trigon structure was formed on the electrode surface and, in the presence of the endonuclease Nb.BbvCI, the (capture probe/auxiliary probe)-duplex is cleaved. After this cleavage, the released miRNA can form another star-trigon with other capture probe molecules producing, in this way, an amplification cycle and a large decrease of the MB electrochemical signal.

2.1.c. Amplification schemes based on DNA displacement reactions

Another amplification strategy was focused on the double-stranded DNA displacement reaction. Wang et al. [33] reported a biosensor for miRNA-24 using a platform of GCE modified by electrodeposition of cobalt oxide petals and poly(o-phenylenediamine) and covalent attachment of hyaluronic acid and methionine-gold nanoclusters as support for the “partial” probe/MB-reporter double strand. Since the sequence of MB-reporter is not exactly complementary to the probe, the miRNA-24 produces the displacement of the MB-reporter with the consequent decrease of MB-amperometric signal.

2.1.d. Amplification schemes based on special nucleic acids structures

Hairpins, molecular beacons, locked nucleic acids, and G-quadruplexes have been also used for the development of miRNAs bioanalytical platforms, taking advantage of the particular properties of each structure. Xue et al. [34] described

the voltammetric and impedimetric attomolar quantification of miRNA-141 using a GCE modified with AuNPs and a hairpin-locked DNAzyme which was opened in the presence of miRNA-141, yielding the “active” DNAzyme that, after cleavage by Mg^{2+} , releases the target and generates successive activation cycles. The remaining fragment on the electrode surface collects numerous CuCo–CeO₂-signaling DNA bioconjugates and, in this way, the biosensing platform offers the great advantage of having two analytical signals, the voltammetric response of the hydrogen peroxide reduction and the charge transfer resistance due to the non-soluble nature of 3,3-diaminobenzidine (DAB) oxidation product. Azzouzi et al. [35] proposed an impedimetric biosensor for sub-pM quantification of micro RNA-21 which relies on the use of GCE modified with neutravidin and a highly specific biotinylated DNA/Locked nucleic acid (LNA) molecular beacon-probe conjugated with AuNPs. The hybridization with miRNA-21 allows the activation of biotin and the collection of the biotinylated multistructure at the glassy carbon platform, decreasing the charge transfer resistance of $[Fe(CN)_6]^{3-/4-}$. Ren et al. [36] reported an electrochemical sensor for non-labeled quantification of miRNA-let-7-a through the formation of trivalent DNAzyme junctions by catalytic hairpin assembly (CHA). The target can lead to CHA of three hairpins into many trivalent DNAzyme junctions that cleave more efficiently the surface G-quadruplex-containing DNA and allow the binding of hemin, with the consequent enhancement of the associated current in the presence of hydrogen peroxide. Miao et al. [37] described a very interesting strategy for the fM detection of miRNA-21 by using sandwich hybridization at a capture probe-modified gold surface, and a signaling probe rich in guanine residues labeled with MB. In the presence of miRNA-21 and K^+ , the

signaling probe is transformed in G-quadruplex, allowing the specific interaction of the Ir(III) complex that works as peroxidase mimics, catalyzing the reduction of hydrogen peroxide, and increasing the voltammetric signal of the redox mediator MB. Huang et al. [38] described a highly sensitive electrochemical biosensor for miRNA which relied on the use of tetrahedral DNA nanostructure probes and guanine nanowire amplification. In the presence of miRNA, the hairpin of one of the branches of the tetrahedral is opened, the stem sequence of the hairpin is released, and the generated G-quadruplex induces the construction of a guanine nanowire. After the addition of hemin, and in the presence of hydrogen peroxide, the G-quadruplex-hemin repeat units catalyzes the oxidation of TMB (Figure 6). An original strategy focused on the use of a bipedal DNA, was proposed for the ratiometric attomolar quantification of exosomal miRNA-21 [39]. The DNA walker released after magnetic separation of streptavidin-magnetic beads/capture DNA/DNA walker/miRNA-21 is dropped at the biorecognition platform of GCE-AuNPs modified by immobilization of a hairpin-MB producing a conformational change in the hairpin-1 that makes possible the hybridization with the hairpin-2 modified with Fc. As a consequence of that, the DNA walker starts to walk and, finally, both redox markers, MB and Fc, remain close to the electrode surface, making easier the charge transfer and increasing the ratio Fc current/MB current with the increment of miRNA-21 concentration.

2.1.e. Amplification schemes based on hybridization chain reaction

Hybridization chain reaction (HCR) is an excellent amplification technique based on the enzyme-free assembly of nucleic acids under isothermal conditions,

at variance with other isothermal amplification techniques like rolling change amplification (RCA), ligase chain reaction (LCR), or the use of nuclease digestion, which need the assistance of specific enzymes. Several strategies have been proposed for the development of HCR-based miRNA biosensors. Cheng et al. [40] reported the enzyme-free amplification for miRNA-21 biosensing using mesoporous silica containers (MSNs), CHA and HCR. The analytical signal was obtained from the SWV signal of the MB released from mesoporous silica nanospheres-hairpin H1 and then intercalated within the duplex generated at the gold electrode/capture-DNA after H1-miRNA-21 hybridization as a consequence of HCR and CHA in the presence of the hairpin H2 (Figure 7). Feng et al. [41] proposed a thiol-hairpin-capture probe modified gold electrode, which suffers a conformational change in the presence of miRNA-21 and triggers HCR to generate a long DNA strand that allows an enhancement in SWV signals of the molybdophosphate generated by accumulation of molybdate at the DNA phosphate residues. Guo et al. [42] described the sub-fM detection of miRNA-21 through the combination of a dual signal amplification strategy that involves HCR to expand the miRNA-21 into a longer structure and provides more sites for the enzyme induced metallization (EIM). The conjugates generated at the magnetic nanobeads modified with the capture probe allowed the association of a high number of conjugates containing ALP, which in the presence of p-aminophenyl phosphate (p-APP) produces p-aminophenol that reduces the Ag^+ deposited at the electrode surface, enhancing the Ag anodic stripping signal (Figure 8A). Figure 8B clearly demonstrates the advantages of the elongation and the labelling of the signaling DNA on the final voltammetric signal of the accumulated Ag. Tian et al.

[43] proposed the determination of microRNA-21 at aM level using a hairpin capture probe immobilized at Fe₃O₄, which is opened after hybridization with miRNA-21 while the exposed portion of the hairpin-capture probe opens two alternating HDNA, propagating a HCR and forming a nicked double helix that allows the accumulation of the planar Cu(II) complex. The analytical signal was obtained through the synergized catalytic reduction of hydrogen peroxide/TMB system due to the action of the copper complex and Fe₃O₄. Liang et al. [44] described a label-free and enzyme-free detection of miRNA-21 at pM levels using an isothermal amplification scheme based on cascade-HCR and different electrochemical transduction approaches, EIS using [Fe(CN)₆]^{3-/4-}, DPV in connection with the intercalation of MB in the hyper-branched resulting dsDNA, and chronocoulometry using RuHex. The miRNA captured at the thiolated biorecognition DNA-modified gold electrode initiates autonomous assembly of DNA nanostructures through the toehold-mediated strand displacement reaction and the resulting cascade HCR, producing the extended growth of DNA chains and higher amplification efficiency compared to the regular HCR.

Yuan et al. [45] reported a biosensor for the simultaneous detection of pancreatic cancer biomarkers, miRNA-141 and miRNA-21, by taking advantage of the use of Fe₃O₄-NPs modified with two different redox markers, thionine (Thi) and ferrocene carboxaldehyde (Fc), and target-triggered HCR. In the presence of the corresponding miRNAs, the thiol-modified hairpin capture probes (HCP1 and HCP2) immobilized at Au, hybridize with miRNA-141 and miRNA-21, leading to the conformational change of these probes that trigger HCR and produce the capture of the signaling DNAs modified with the redox markers. The increase in the DPV

currents associated with the oxidation of the redox markers allowed the simultaneous quantification of miR-141 and miR-21, with successful application in cell lysates. Bao et al. [46] proposed an interesting alternative for miRNA-16-amplified biosensing through the association of a nanocomposite platform to build the biorecognition layer, CHA to obtain the double helix, and HCR to elongate the DNA strands and facilitate the intercalation of the redox marker. The bioanalytical platform was obtained by integrating AuNPs/polypyrrole-reduced GO (Au/PPy-rGO) at GCE to amplify the electrochemical signal and to support the thiolated capture probe (Figure 9 A and B). The final electrochemical transduction was performed by DPV of the intercalated MB as indicated in Figure 9C. The corresponding calibration plot is depicted in Figure 9D, with a very wide linear range and a fM detection of miRNA-16.

2.1.f. Amplification schemes based on catalyzed hairpin assembly

Zhang K. et al. [47] proposed the combination of a supramolecular sensing architecture based on ZrO₂-RGO modified electrode and CHA for the very sensitive detection of miRNA-21. The platform was obtained by immobilization of ZrO₂-RGO, followed by the covalent attachment of the capture RNA (hairpin 1), which, in the presence of the target, hybridizes and opens the hairpin H2, releasing the miRNA and allowing the incorporation of H2 to the electrode in a cyclic way through CHA. The amplified charge transfer resistance of [Fe(CN)₆]^{3-/4-} was used as analytical signal allowing the detection of fM levels. Li et al. [48] proposed a ratiometric scheme based on target driven CHA mismatched using three hairpins, H1, Fc-H2 with 2 mismatches and a thiolated-H3 modified with MB immobilized at

the gold electrode. Due to the mismatches, the hybridization between H1 and H2 is not very efficient, and in the presence of the target miRNA-21, the strand displacement occurs, exposing the portion complementary to H2, and allowing the H1-H2 hybridization. In this way, miRNA-21 is released and cyclically hybridizes with more H1. Finally, the exposed portion of H1-H2 duplex hybridizes with H3, leaving the MB far away and Fc close to the electrochemical interface, making possible the fM detection of the hybridization from the increment in the voltammetric signal of Fc and the decrease of the MB one (Figure 10).

2.1.g. Other amplification schemes

Mandli et al. [49] proposed the use of sandwich hybridization onto AuNPs-modified PGE and the detection using a conjugate ALP-Streptavidin from the naphthol oxidation signal in the presence of α -naphthyl phosphate. Deng et al. [50] described a sandwich hybridization between capture DNA-AuNPs, miRNA-21 and MWCNTs modified with a signaling DNA and labeled with thionine. Therefore, the presence of miRNA-21 was determined from the voltammetric signal of thionine, which increases with the concentration of the target, being the detection limit 0.032 pM. Liu et al. [51] reported a sandwich electrochemical exosomal microRNA-21 sensor (SEEmiR) using peptide nucleic acid as biorecognition element and spherical DNA (SNA) as secondary probe. The hybridization signal was obtained from the chronocoulometric response of RuHex, with a detection limit of 49 aM (Figure 11A). The increment of the voltammetric and chronocoulometric signals for RuHex in the presence of SNA clearly demonstrate the importance of the SNA-mediated amplification (Figure 11B). These advantages are also evident from the calibration plots depicted in Figure 11C. This ultrasensitive sensor allows the label-

free and enzyme-independent miRNA detection in cell lysates, unpurified tumor exosomal lysates and blood of cancer patients.

A simple scheme was recently described by Zouari et al. [52] for the quantification of miRNA-21 at fM level through the sandwich hybridization between the thiolated-DNA probes at SPCE modified with GO-AuNPs nanohybrid and the signaling DNA conjugated with Fc-AuNPs-Streptavidin, being Fc the responsible of the analytical signal (Figure 11).

Zhang C. et al. [53] described the attomolar and label-free electrochemical miRNA-21 biosensor based on RCA that produces a massive G-rich long ssDNA to be used as matrix for the *in situ* synthesis of PdNPs based on the interaction of Pd(II) with the nitrogen atoms of guanine residues, enhancing the electrochemical signal.

Vargas et al. [54] reported an innovative amperometric magneto-biosensor for the sub-pM detection of miRNA-21 by combining geno- and immunoassays through the use of magnetic beads modified with streptavidin as platform and detection at a magneto SPCE through the use of an anti DNA-RNA antibody and the bacterial protein A (ProtA) conjugated with a horseradish peroxidase (HRP) homopolymer (Poly-HRP40) as an enzymatic label for signal amplification in the presence of hydrogen peroxide and hydroquinone.

Cao et al. [55] proposed an electrochemical biosensor for the simultaneous detection of miRNA-155 and miRNA-122 based on covalent-organic framework (COF) nanowire synthesized via condensation polymerization of 1,3,6,8-tetra(4-carboxylphenyl)pyrene and melamine (TBAPy-MA-COF-COOH) as platform for immobilizing the capture ssDNAs able to hybridize with the aptamers

anti-miRNA155 and anti-miRNA-22 modified with shell-encoded AuNPs as signal labels (AgNCs@AuNPs and Cu₂O@AuNPs, respectively). In the presence of miRNA-122 and miRNA-155, the aptamers recognize them and are released from the electrode surface, with the consequent decrease in the DPV peak current density at -0.1 V (Cu₂O@AuNPs) and 0.08 V (AgNCs@AuNPs) allowing the detection of fM and sub-pM levels for miRNA 155 and miRNA 122, respectively.

2.1.h. Concluding remarks about amplification-based schemes

The analysis of the different amplification-based approaches for electrochemical miRNAs biosensing previously discussed, clearly demonstrate that, in general, and depending on the strategy, is possible to reach detection limits at sub-fM levels with relatively simple schemes, without involving enzymes or additional reactions, just using the electrochemical signal due to an electrostatically accumulated redox marker at the surface of adsorbed miRNA or surface-generated heteroduplex, with or without additional catalytic cycles. The association of endonucleases with electrochemical transduction, either using redox markers or enzymatic labelling, represents a very successful alternative to get more sensitive quantification of miRNAs, with extremely low detection limits in some of the approaches. However, is also important to remark that, at the same time that the system can be pushed-down to lower detection levels, these assay time considerably increases due to the higher number of steps involved in the protocol. Similar behavior is observed when using special structures of nucleic acids or analogues, HCR, CHA, RCA, either alone or combined, associated with metallic

complexes, metallic nanostructures or redox markers. The multiple possibilities to combine the signaling DNAs and/or markers gives to these strategies a great potential and the advantage of reaching extremely low detection limits.

Nevertheless, as in the case of endonucleases-based protocols, despite the improved sensitive and selectivity, the processes are time-consuming. The simplest scheme is the sandwich hybridization, being the rational selection of the signaling probe label the most critical aspect to guarantee a good analytical performance. Thus, although the detection limits are not as low as in the other amplification-based protocols, their analytical characteristics of the sandwich hybridization schemes are very useful for the quantification of miRNAs in real samples, with the great advantage of the lower number of steps and shorter assay-time.

2.2. Non-amplified electrochemical miRNAs biosensors

The results discussed in the previous section demonstrated that amplification-based electrochemical miRNAs biosensors present clear advantages mainly connected to the sensitivity and the possibility to reach extremely low detection limits, essential condition to detect circulating miRNAs. However, in spite of the excellent analytical performance of these biosensors, the search for simple, sensitive, and selective miRNA biosensing schemes, that allow the faster, cheaper and easier quantification of miRNAs is still receiving great attention. In this section we discuss the most representative non-amplified electrochemical miRNAs biosensors.

One interesting strategy has been the development of ratiometric biosensors focused on the electrochemical response of two redox markers, which was dependent on the distance from the electrode before and after the hybridization event. In this direction, Luo et al. [56] proposed the non-amplified fM ratiometric-detection of exosomal miRNA-21 based on the currents ratio of MB and Fc located in Y shape-like probe (generated at the polylysine-modified GCE) through the locked-nucleic acid (LNA)-assisted strand displacement reaction that takes place in the presence of the target (Figure 12).

Pingarrón's group reported an innovative biosensing scheme based on the competitive RNA-RNA hybridization using a AuNPs-modified SPCE as platform for the immobilization of capture RNA probe. The analytical signal was obtained from the changes in the amperometric response of the hydrogen peroxide/hydroquinone system which was dependent on the amount of streptavidin-HRP conjugate associated to the supramolecular architecture obtained after the competition between biotinylated-miRNA-21 and the target miRNA-21 (Figure 13) [57].

Kaplan et al. [58] described the use of PGE modified with the DNA probe entrapped in a matrix of electropolymerized polypyrrole for the non-labeled detection of miRNA-21 either, from the change in the charge transfer resistance of $[\text{Fe}(\text{CN})_6]^{3-/4-}$ or from the voltammetric reduction signal of the Meldola blue redox marker, with successful application in a breast cancer cell line. Another non-labeled biosensing platform based on the use of PGE was proposed for the ppb level quantification of miRNA-660. It relied on the immobilization of a CHIT/nitrogen doped-RGO composite to support the probe and the transduction of the hybridization event from the change in the charge transfer resistance of the redox

marker $[\text{Fe}(\text{CN})_6]^{3-/4-}$ [59]. Su et al. [60] described the sub-fM detection of miRNA-21 using indium tin oxide (ITO) modified with hierarchical flower-like AuNPs as platform for the capture probe immobilization and voltammetric detection of the RuHex accumulated after hybridization, with successful application in human lung cancer cell (A549) lysates and serum. Bharti et al. [61] proposed a bioanalytical platform of fluorine tin oxide (FTO) modified with carboxylated-GO, electrodeposited AuPt-NPs and streptavidin to allow the anchorage of the biotinylated probe and the detection of miRNA-21 biorecognition event through the decrease of $[\text{Fe}(\text{CN})_6]^{3-/4-}$ DPV signal.

Su et al. [62] proposed the detection of miRNA-21 at fM level through the changes in the redox signal of MB at GCE containing MB-modified MoS_2 before and after the formation of the DNA-miRNA-21 heteroduplex. Wang F. et al. [63] reported the fM detection of the hepatocellular carcinoma biomarker miRNA-122 using Au modified with a thiolated-DNA probe, GO adsorbed through π -stacking and Prussian blue (PB) grown *in situ* at the GO layer. The analytical signal was obtained from the decrease of PB voltammetric response in the presence of miRNA, due to the differential affinity of GO with ssDNA and DNA-RNA. Following a similar scheme, Zhu et al. [64] reported the label-free and simple detection of miRNA-21, through the decrease of the SWV signal of thionin after hybridization with miRNA-21 at a GCE/ MoS_2 -thionine-AuNPs. Tran et al. [65] reported a label-free and reagentless sensing of miRNA based on the use of a DNA probe-AuNPs-modified GCE and 5-hydroxy-3-hexanedithiol-1,4-naphthoquinone, as indicator of the analytical signal. Tian et al. [66] proposed another label-free strategy that allowed the highly sensitive and simple electrochemical miRNA biosensing by

using polypyrrole-coated AuNPs as platform to immobilize the RNA probe, evaluating the hybridization event from the DPV oxidation signal of toluidine blue (TB) preferentially accumulated at the duplex. Kaugkamano et al. [67] described the voltammetric detection of miRNA-21 at fM levels through the decrease of Ag oxidation signal at Au modified with electropolymerized polypyrrole/Ag nanofoam and pyrrolidinyI-PNA as biorecognition element. Jeong et al. [68] presented the label-free quantification of miR-375 at aM level in pure buffer solution and fM level in metastatic prostate cancer cells using a simple non-amplified electrochemical transduction. The biosensing strategy was obtained by immobilization of a thiolated capture probe at Au followed by the hybridization and electrochemical transduction using the $[\text{Fe}(\text{CN})_6]^{3-/4-}$ SWV response.

These amplification-free miRNAs electrochemical biosensors, allows us to conclude that is possible to obtain a sensitive miRNA quantification even without amplification steps, greatly simplifying the analytical procedure and reducing the cost and the time of the assay. These biosensors present figures of merit really competitive compared to those based on amplification schemes, making them very interesting for several applications, like the implementation in low-resources settings.

3. Conclusions and Perspectives

The last years have witnessed a notable growth of the miRNA-biosensors field due to the increased knowledge of the clinical usefulness of miRNAs as biomarkers for the diagnosis, prognosis, and even therapy of relevant diseases, some of them responsible for the highest death-percentage of the population, like

cancer and cardiovascular diseases. This review summarized the most significant achievements in the development of electrochemical biosensors for the quantification of miRNAs reported between 2017 and the beginning of 2020.

The electrochemical miRNA-biosensors presented here involve different probes (RNAs, conventional DNAs, hairpins, walker and tetrahedral DNAs, DNAs analogues), immobilized at diverse electrodes (GCE, PGE, SPCE, Au, ITO, FTO), combined with different nanomaterials (MoS₂, CNTs, graphene derivatives, AuNPs, metallic nanoparticles) and nanomagnetic separation, associated with a variety of biorecognition/transduction strategies (sandwich hybridization; use of redox markers; labelled redox enzymes; isothermal amplification schemes like HCR, CHA, RCA; endonucleases-based and strand displacement reactions), in connection with impedimetric, voltammetric, chronocoulometric or (chrono)amperometric detection.

Even when the different amplification alternatives demonstrate clear advantages, the efficiency of non-amplified miRNA biosensing is also remarkable considering that they offer not only faster, simpler and cheaper quantification, but also analytical competitiveness. Further developments should consider the design of novel bioreceptors and new signaling schemes involving aptamers, lectins or antibodies with improved specificity towards RNA-DNA heteroduplexes.

Most of the electrochemical miRNA-biosensors have demonstrated to be successful in biological fluids and cell lysates; however, one important aspect that requires special attention for the real clinical application of these biosensors and further incorporation in routine analysis, is the evaluation of a large cohort of patients. In this way, it would be possible to demonstrate that the biosensor

successfully works even for patients with different coexisting pathologies, diverse health-state and under administration of a variety of medicines. The incorporation of under-expressed miRNAs like tumor suppressors in the battery of targets for electrochemical miRNA-biosensors is another important challenge that should be considered for further developments. Taking into account that, in general, the known miRNAs are not specific only for one pathology, special attention should be also paid to the development of electrochemical biosensors devoted to the simultaneous quantification of a panel of miRNAs to facilitate the diagnosis with improved reliability.

In summary, the electrochemical miRNA-biosensors field is flourishing, and has demonstrated an incredible evolution in the last decade in consonance with the increasing studies of basic aspects about the role of miRNAs. The new efforts and the new challenges should be focused on the development of point-of-care devices able to address the requirements of the new dimensions of diagnosis in the Medicine of the future, overcoming the limitations in terms of portability, cost, and easy adaptability to a broad range of settings.

CONFLICTS OF INTEREST

On behalf of the authors of the manuscript “**New trends in the development of electrochemical biosensors for the quantification of microRNAs**” by López Mujica, Gallay, Perrachione, Montemerlo, Tamborelli, Vaschetti, Reartes, Bollo, Rodríguez, Dalmasso, Rubianes and Rivas, I declare that there are no conflicts of interest

Acknowledgements

Financial support from CONICET, ANPCyT, SECyT-UNC. M. L. M. thankfully acknowledges ANPCyT for the PhD fellowship. P. A. G., V. V., L. A. T., D. R., and A. E. M acknowledge CONICET for the fellowships.

References

- [1] K. Wolska-Gawron, J. Bartosińska, D. Krasowska. MicroRNA in localized scleroderma: a review of literature. *Arch. Dermatol. Res.* 312 (2020) 317–324.
- [2] N. Bushati, S.M. Cohen. MicroRNA functions. *Annu. Rev. Cell Dev. Biol.* 23 (2007) 175–205.
- [3] C. Catalanotto, C Cogoni, G Zardo. MicroRNA in control of gene expression: an overview of nuclear functions. *Int J Mol Sci.* 17 (2016) 1712.
- [4] M.M.H. Sohel. Circulating microRNAs as biomarkers in cancer diagnosis. *Life Sci.* 248 (2020) 117473.
- [5] A.H. Harrill, A.P. Sanders. Urinary MicroRNAs in Environmental Health: Biomarkers of Emergent Kidney Injury and Disease. *Curr. Environ. Health Rep.* 7 (2020) 101–108.
- [6] T. Machackova, V. Prochazka, Z. Kala, O. Slaby. Translational Potential of microRNAs for preoperative Staging and Prediction of Chemoradiotherapy Response in Rectal Cancer. *Cancers* 11 (2019) 1545.
- [7] A.A. Hembrom, S. Srivastava, I. Garg, B. Kumar. MicroRNAs in venous thrombo-embolism. *Clin. Chim. Acta* 504 (2020) 66–72.

- [8] X. Kou, D. Chen, N. Chen. The Regulation of microRNAs in Alzheimer's. *Front. Nuerol.* 11 (2020) 288.
- [9] J.S. Ghizoni, R. Nichele, M.T. de Oliveira, S. Pamato, J.R. Pereira. The utilization of saliva as an early diagnostic tool for oral cancer: microRNA as a biomarker. *Clin. Transl. Oncol.* 22 (2020) 804–812.
- [10] D. Bidarra, V. Constâncio, D. Barros-Silva, J. Ramalho-Carvalho, C. Moreira-Barbosa, L. Antunes, J. Maurício, J. Oliveira, R. Henrique, C. Jerónimo. Circulating MicroRNAs as Biomarkers for Prostate Cancer Detection and Metastasis Development Prediction. *Front. Oncol.* 9 (2019) 900.
- [11] M. Russano, A. Napolitano, G. Ribelli, M. Iuliani, S. Simonetti, F. Citarella, F. Pantano, E. Dell'Aquila, C. Anesi, N. Silvestris, A. Argentiero, A. Solimando, B. Vincenzi, G. Tonini, D. Santin. Liquid biopsy and tumor heterogeneity in metastatic solid tumors: the potentiality of blood samples. *J. Exp. Clin. Cancer Res.* 39 (95) (2020).
- [12] Z. Wang, B. Yang. Northern Blotting and Its Variants for Detecting Expression and Analyzing Tissue Distribution of miRNAs. *MicroRNA Expression Detection Methods.* Springer, Berlin Heidelberg (2010) 83–100.
- [13] S. Rosenwald, S. Gilad, S. Benjamin, D. Lebanony, N. Dromi, A. Faerman, H. Benjamin, R. Tamir, M. Ezagouri, E. Goren, I. Barshack, D. Nass, A. Tobar, M. Feinmesser, N. Rosenfeld, I. Leizerman, K. Ashkenazi, Y. Spector, A. Chajut, R. Aharonov. Validation of a microRNA-based qRT-PCR test for accurate identification of tumor tissue origin. *Mod. Pathol.* 23 (2010) 814-823.
- [14] H. Konishi, D. Ichikawa, S. Komatsu, A. Shiozaki, M. Tsujiura, H. Takeshita, R. Morimura, H. Nagata, T. Arita, T. Kawaguchi, S. Hirashima, H. Fujiwara, K.

- Okamoto, E. Otsuji. Detection of gastric cancer-associated microRNAs on microRNA microarray comparing pre- and post-operative plasma. *Br. J. Cancer* 106 (2012) 740–747.
- [15] M. López-Mujica, Y. Zhang, F. Bedioui, F. Gutierrez, G. Rivas. Label-free graphene oxide based-SPR genosensor for the quantification of microRNA21. *Anal. Bioanal. Chem.* 412 (2020) 3539-3546.
- [16] T. Kilica, A. Erdemb, M. Ozsozb, S. Carrara. MicroRNA biosensors: Opportunities and challenges among conventional and commercially available techniques. *Biosens. Bioelectron.* 99 (2018) 525–546.
- [17] P. Gillespie, S. Ladame, D. O'Hare. Molecular methods in electrochemical microRNA detection. *Analyst* 144 (2019) 114-129.
- [18] K. Mahato, A. Kumar, P.K. Maurya, P. Chandra. Shifting paradigm of cancer diagnoses in clinically relevant samples based on miniaturized electrochemical nanobiosensors and microfluidic devices. *Biosens. Bioelectron.* 100 (2018) 411-428.
- [19] J. Das, S.O. Kelley. High-Performance Nucleic Acid Sensors for Liquid Biopsy Applications. *Angewandte Chemie - International Edition* 59 (2020) 2554-2564.
- [20] M.K. Masud, M. Umer, M.S.A. Hossain, Y. Yamauchi, N.T. Nguyen, M.J.A. Shiddiky. Nanoarchitecture Frameworks for Electrochemical miRNA Detection. *Trends Biochem. Sci.* 44 (2109) 433-452.
- [21] M. Bartosik, L. Jirakova. Electrochemical analysis of nucleic acids as potential cancer biomarkers. *Curr. Opin. Electrochem.* 14 (2019) 96-103.
- [22] M.N. Islam, L. Gorgannezhad, M.K. Masud, S. Tanaka, M.S.A, Hossain, Y. Yamauchi, N.T. Nguyen, M.J.A. Shiddiky. Graphene-Oxide-Loaded

Superparamagnetic Iron Oxide Nanoparticles for Ultrasensitive Electrocatalytic Detection of MicroRNA. *ChemElectroChem* 5 (2018) 2488-2495.

[23] M.N. Islam, M.K. Masud, N.T. Nguyen, V. Gopalan, H.R. Alamri, Z.A.

Allothman, M.S.A. Hossain, Y. Yamauchi, A.K.Y. Lam, M.J.A. Shiddiky. Gold-loaded nanoporous ferric oxide nanocubes for electrocatalytic detection of microRNA at attomolar level. *Biosens. Bioelectron.* 101 (2018) 275-281.

[24] S. Su, W. Cao, W. Liu, Z. Lu, D. Zhu, J. Chao, L. Weng, L. Wang, C. Fan, L. Wang. Dual-mode electrochemical analysis of microRNA-21 using gold nanoparticle-decorated MoS₂ nanosheet. *Biosens. Bioelectron.* 94 (2017) 552-559.

[25] A. Ganguly, J. Benson, P. Papakonstantinou. Sensitive chronocoulometric detection of miRNA at SPCE modified by gold-decorated MoS₂ nanosheets. *ACS Appl. Bio. Mater.* 1 (2018) 1184-1194.

[26] A.D. Castañeda, N.J. Brenes, A. Kondajji, R.M. Crooks. Detection of microRNA by electrocatalytic amplification: a general approach for single-particle, biosensing. *J. Am. Chem. Soc.* 139 (2017) 7657-7664.

[27] P. Miao, Y. Tang, B. Wang, C. Jiang, L. Gao, B. Bo, J. Wang. Nuclease assisted target recycling and spherical nucleic acids gold nanoparticles recruitment for ultrasensitive detection of microRNA. *Electrochim. Acta* 190 (2016) 396-401.

[28] B. Bo, T. Zhang, Y. Jiang, H. Cui, P. Miao, P. Triple Signal Amplification Strategy for Ultrasensitive Determination of miRNA Based on Duplex Specific Nuclease and Bridge DNA-Gold Nanoparticles. *Anal. Chem.* 90 (2018) 2395-2400.

[29] Y. Tao, D. Yin, M. Jin, J. Fang, T. Dai, Y. Li, Y. Li, Q. Pu, G. Xie. Double-loop hairpin probe and doxorubicin-loaded gold nanoparticles for the ultrasensitive electrochemical sensing of microRNA. *Biosens. Bioelectron.* 96 (2017) 99-105.

- [30] H. Zhang, M. Fan, J. Jiang, Q. Shen, C. Cai, J. Shen. Sensitive electrochemical biosensor for MicroRNAs based on duplex-specific nuclease-assisted target recycling followed with gold nanoparticles and enzymatic signal amplification. *Anal. Chim. Acta* 1064 (2019) 33-39.
- [31] J. Wang, J. Lu, S. Dong, N. Zhu, E. Gyimah, K. Wang, Y. Li, Z. Zhang. An ultrasensitive electrochemical biosensor for detection of microRNA-21 based on redox reaction of ascorbic acid/iodine and duplex-specific nuclease assisted target recycling. *Biosens. Bioelectron.* 130 (2019) 81-87.
- [32] P. Miao, B. Wang, Z. Yu, J. Zhao, Y. Tang. Ultrasensitive electrochemical detection of microRNA with star trigon structure and endonuclease mediated signal amplification. *Biosens. Bioelectron.* 63 (2015) 365-370.
- [33] W. Wang, S. Jayachandran, M. Li, S. Xu, X. Luo. Hyaluronic acid functionalized nanostructured sensing interface for voltammetric determination of microRNA in biological media with ultra-high sensitivity and ultra-low fouling. *Microchim. Acta* 185 (2018) 156.
- [34] S. Xue, Q. Li, L. Wang, W. You, J. Zhang, R. Che. Copper- and Cobalt-Codoped CeO₂ Nanospheres with Abundant Oxygen Vacancies as Highly Efficient Electrocatalysts for Dual-Mode Electrochemical Sensing of MicroRNA. *Anal. Chem.* 91 (2019) 2659–2666.
- [35] S. Azzouzi, W.C. Mak, K. Kor, A.P.F. Turner, M.B. Ali, V. Beni. An integrated dual functional recognition/amplification bio-label for the one-step impedimetric detection of Micro-RNA-21. *Biosens. Bioelectron.* 92 (2017) 154-161.

- [36] R. Ren, Q. Bi, R. Yuan, Y. Xiang. An efficient, label-free and sensitive electrochemical miRNA sensor based on target-initiated catalytic hairpin assembly of trivalent DNAzyme junctions. *Sensor Actuat. B-Chem.* 304 (2020) 127068.
- [37] X. Miao, W. Wang, T. Kang, J. Liu, K.K. Shiu, C.H. Leung, D.L. Ma. Ultrasensitive electrochemical detection of miRNA-21 by using an iridium(III) complex as catalyst. *Biosens. Bioelectron.* 86 (2016) 454-458.
- [38] Y.L. Huang, S. Mo, Z.F. Gao, J.R. Chen, J.L. Lei, H.Q. Luo, N.B. Li. Amperometric biosensor for microRNA based on the use of tetrahedral DNA nanostructure probes and guanine nanowire amplification. *Microchim. Acta* 184 (2017) 2597-2604.
- [39] J. Zhang, L.L. Wang, M.F. Hou, Y.K. Xia, W.H. He, A. Yan, Y.P. Weng, L.P. Zeng, J.H. Chen. A ratiometric electrochemical biosensor for the exosomal microRNAs detection based on bipedal DNA walkers propelled by locked nucleic acid modified toehold mediate strand displacement reaction. *Biosens. Bioelectron.* 102 (2018) 33-40.
- [40] H. Cheng, W. Li, S. Duan, J. Peng, J. Liu, W. Ma, H. Wang, X. He, K. Wang. Mesoporous Silica Containers and Programmed Catalytic Hairpin Assembly/Hybridization Chain Reaction Based Electrochemical Sensing Platform for MicroRNA Ultrasensitive Detection with Low Background. *Anal. Chem.* 91 (2019) 10672-10678.
- [41] K. Feng, J. Liu, L. Deng, H. Yu, M. Yang. Amperometric detection of microRNA based on DNA-controlled current of a molybdophosphate redox probe and amplification via hybridization chain reaction. *Microchim. Acta* 185 (2018) 28.

- [42] W.J. Guo, Z. Wu, X.Y. Yang, D.W. Pang, Z.L. Zhang. Ultrasensitive electrochemical detection of microRNA-21 with wide linear dynamic range based on dual signal amplification. *Biosens. Bioelectron.* 131 (2019) 267-273.
- [43] L. Tian, J. Qi, O. Oderinde, C. Yao, W. Song, Y. Wang. Planar intercalated copper (II) complex molecule as small molecule enzyme mimic combined with Fe₃O₄ nanozyme for bienzyme synergistic catalysis applied to the microRNA biosensor. *Biosens. Bioelectron.* 110 (2018) 110-117.
- [44] M. Liang, M. Pan, J. Hu, F. Wang, X. Liu. Electrochemical Biosensor for MicroRNA Detection Based on Cascade Hybridization Chain Reaction. *ChemElectroChem* DOI: 10.1002/celec.201800255.
- [45] Y.H. Yuan, Y.D. Wu, B.Z. Chi, S.H. Wen, R.P. Liang, J.D. Qiu. Simultaneously electrochemical detection of microRNAs based on multifunctional magnetic nanoparticles probe coupling with hybridization chain reaction. *Biosens. Bioelectron.* 97 (2017) 325-331.
- [46] J. Bao, C. Hou, Y. Zhao, X. Geng, M. Samalo, H. Yang, M. Bian, D. Huo. An enzyme-free sensitive electrochemical microRNA-16 biosensor by applying a multiple signal amplification strategy based on Au/PPy-rGO nanocomposite as a substrate. *Talanta* 196 (2019) 329-336.
- [47] K. Zhang, N. Zhang, L. Zhang, H. Wang, H. Shi, Q. Liu. Label-free impedimetric sensing platform for microRNA-21 based on ZrO₂-reduced graphene oxide nanohybrids coupled with catalytic hairpin assembly amplification. *RSC Adv.* 8 (2018) 16146-16151

- [48] X. Li, B. Dou, R. Yuan, Y. Xiang. Mismatched catalytic hairpin assembly and ratiometric strategy for highly sensitive electrochemical detection of microRNA from tumor cells. *Sensor Actuat. B-Chem.* 286 (2019) 191-197.
- [49] J. Mandli, H. Mohammadi, A. Amine. Electrochemical DNA sandwich biosensor based on enzyme amplified microRNA-21 detection and gold nanoparticles. *Bioelectrochemistry* 116 (2017) 17-23.
- [50] K. Deng, X. Liu, C. Li, H. Huang. Sensitive electrochemical sensing platform for microRNAs detection based on shortened multi-walled carbon nanotubes with high-loaded thionin. *Biosens. Bioelectron.* 117 (2018) 168-174.
- [51] L. Liu, H. Lu, R. Shi, X.X. Peng, Q. Xiang, B. Wang, Q.Q. Wan, Y. Sun, F. Yang, G.J. Zhang. Synergy of Peptide-Nucleic Acid and Spherical Nucleic Acid Enabled Quantitative and Specific Detection of Tumor Exosomal MicroRNA. *Anal. Chem.* 91 (2019) 13198-13205.
- [52] M. Zouari, S. Campuzano, J.M. Pingarrón, N. Raouafi. Femtomolar direct voltammetric determination of circulating miRNAs in sera of cancer patients using an enzymeless biosensor. *Anal. Chim. Acta* 1104 (2020) 188-198.
- [53] C. Zhang, D. Li, D. Li, K. Wen, X. Yang, Y. Zhu. Rolling circle amplification-mediated: In situ synthesis of palladium nanoparticles for the ultrasensitive electrochemical detection of microRNA. *Analyst* 144 (2019) 3817-3825.
- [54] E. Vargas, R.M. Torrente-Rodríguez, V.R.V. Montiel, E. Povedano, M. Pedrero, J.J. Montoya, S. Campuzano, J.M. Pingarrón. Magnetic beads-based sensor with tailored sensitivity for rapid and single-step amperometric determination of miRNAs. *Int. J. Mol. Sci.* 18 (2017) 2151.

- [55] Z. Cao, F. Duan, X. Huang, Y. Liu, N. Zhou, L. Xia, Z. Zhang, M. Du. A multiple aptasensor for ultrasensitive detection of miRNAs by using covalent-organic framework nanowire as platform and shell-encoded gold nanoparticles as signal labels. *Anal. Chim. Acta* 1082 (2019) 176-185.
- [56] L. Luo, L. Wang, L. Zeng, Y. Wang, Y. Weng, Y. Liao, T. Chen, Y. Xia, J. Zhang, J. Chen. A ratiometric electrochemical DNA biosensor for detection of exosomal MicroRNA. *Talanta* 207 (2020) 120298.
- [57] M. Zouari, S. Campuzano, J.M. Pingarrón, N. Raouafi. Competitive RNA-RNA hybridization-based integrated nanostructured-disposable electrode for highly sensitive determination of miRNAs in cancer cells. *Biosens. Bioelectron.* 91 (2017) 40-45.
- [58] M. Kaplan, T. Kilic, G. Guler, J. Mandli, A. Amine, M. Ozsoz. A novel method for sensitive microRNA detection: Electropolymerization based doping. (2017) *Biosens. Bioelectron.* 92 (2017) 770-778.
- [59] E. Eksin, S.K. Bikkarolla, A. Erdem, P. Papakonstantinou. Chitosan/Nitrogen Doped Reduced Graphene Oxide Modified Biosensor for Impedimetric Detection of microRNA. *Electroanalysis* 30 (2018) 551-560.
- [60] S. Su, Y. Wu, D. Zhu, J. Chao, X. Liu, Y. Wan, Y. Su, X. Zuo, C. Fan, L. Wang. On-Electrode Synthesis of Shape-Controlled Hierarchical Flower-Like Gold Nanostructures for Efficient Interfacial DNA Assembly and Sensitive Electrochemical Sensing of MicroRNA. *Nano Micro Small* 12 (2016) 3794-3801.
- [61] A. Bharti, N. Agnihotri, N. Prabhakar. A voltammetric hybridization assay for microRNA-21 using carboxylated graphene oxide decorated with gold-platinum bimetallic nanoparticles. *Microchim. Acta* 186 (2019) 185.

- [62] S. Su, Q. Hao, Z. Yan, R. Dong, R. Yang, D. Zhu, J. Chao, Y. Zhou, L. Wang. A molybdenum disulfide@Methylene Blue nanohybrid for electrochemical determination of microRNA-21, dopamine and uric acid. *Microchim. Acta* 186 (2019) 607.
- [63] F. Wang, Y. Chu, Y. Ai, L. Chen, F. Gao F. Graphene oxide with in-situ grown Prussian Blue as an electrochemical probe for microRNA-122. *Microchim. Acta* 186 (2019) 116.
- [64] D. Zhu, W. Liu, D. Zhao, Q. Hao, J. Li, J. Huang, J. Shi, J. Chao, S. Su, L. Wang. Label-Free Electrochemical Sensing Platform for MicroRNA-21 Detection Using Thionine and Gold Nanoparticles Co-Functionalized MoS₂ Nanosheet. *ACS Appl. Mater. Interfaces* 9 (2017) 35597-35603.
- [65] H.V. Tran, N.D. Nguyen, B. Piro, L.T. Tran. Fabrication of a quinone containing layer on gold nanoparticles directed to a label-free and reagentless electrochemical miRNA sensor. *Anal. Methods* 9 (2017) 2696-2702.
- [66] L. Tian, K. Qian, J. Qi, Q. Liu, C. Yao, W. Song, Y. Wang. Gold nanoparticles superlattices assembly for electrochemical biosensor detection of microRNA-21. *Biosens. Bioelectron.* 99 (2018). 564-570.
- [67] T. Kangkamano, A. Numnuam, W. Limbut, P. Kanatharana, T. Vilaivan, P. Thavarungkul. PyrrolidinyI PNA polypyrrole/silver nanofoam electrode as a novel label-free electrochemical miRNA-21 biosensor. *Biosens. Bioelectron.* 102 (2018) 217-225.
- [68] B. Jeong, Y.J. Kim, J.Y. Jeong, Y.J. Kim. Label-free electrochemical quantification of microRNA-375 in prostate cancer cells. *J. Electroanal. Chem.* 846 (2019) 113127.

LEGENDS OF THE FIGURES

Figure 1. Nuclear and cytoplasmic processing of miRNAs and mechanisms of gene expression regulation. Reprinted from Ref. [4], Copyright (2020), with permission from Elsevier.

Figure 2. Schematic of label-free and dual mode electrochemical assay for miRNA-21 detection based on gold-nanoparticle-decorated MoS₂ nanosheet. Reprinted from Ref. [24], Copyright (2017), with permission from Elsevier.

Figure 3. Scheme of the amplified detection of miRNA through the activity of DSN and the accumulation of the redox marker RuHex. Reprinted from Ref. [27], Copyright (2016), with permission from Elsevier.

Figure 4. Scheme for the triple amplified detection of miRNA with electrochemical quantification through the accumulation of the redox marker RuHex. Reprinted with permission from Ref. [28], Copyright (2018), American Chemical Society.

Figure 5. A) Scheme of the electrochemical miRNA biosensor based on DSN-assisted target recycling followed with AuNPs and HRP enzymatic signal amplification strategy. B) Cyclic voltammograms of the electrochemical biosensor monitoring the TMB redox reaction in the presence of: a) 0M, b) 100 fM, c) 100 pM miRNA-21. C) Chronoamperometric signals obtained for different concentrations of miRNA-21 a) to i) is 0.01fM, 1fM, 10 fM, 50 fM, 100 fM, 1 pM, 10 pM, 100, pM, respectively. The inset is the linear calibration plot of Δi versus the logarithm of miRNA-21 concentration. Adapted from Ref. [30], Copyright (2019), with permission from Elsevier.

Figure 6. Schematic representation for the different steps during the building of the electrochemical miRNA biosensor and the electrochemical transduction. Adapted by permission from Springer Nature: Amperometric biosensor for microRNA based on the use of tetrahedral DNA nanostructure probes and guanine nanowire amplification, Huang, Y.L., Mo, S., Gao, Z.F., Chen, J.R., Lei, J.L., Luo, H.Q., Li, N.B., Copyright (2017)

Figure 7. (A) Schematic diagram of MSNs and programmed CHA/HCR based electrochemical sensing platform for miRNA-21 ultrasensitive detection. **(B)** SWV

response of the programmed CHA/HCR on SH-CP/MCH-modified AuE incubated with the mixtures of (a) MB@MSNs-DNA, H1, H2, and H4 probes, (b) target miRNA-21, MB@MSNs-DNA, and H2 probe, and (c) target miRNA-21, MB@MSNs-DNA, H2, H3, and H4 probes. MSNs, mesoporous silica containers; CHA, catalytic hairpin assembly; HCR, hybridization chain reaction; CP, capture probe; MCH, 6-mercaptophexanol; MB, methylene blue. Adapted with permission from Ref. [40]. Copyright 2019 American Chemical Society.

Figure 8. (A) Schematic diagram of the protocol for electrochemical detection of miRNA-21: capture of miRNA-21 and HCR (above), and EIM and electrochemical detection of multiple samples on the same MA (below). **(B)** LSVs under different conditions: MBs / CP H1 / miRNA-21 / biotin-H2 (curve black), MBs / CP H1 / miRNA-21 / biotin-H2 / SA-ALP (curve red), and MBs / CP H1 / miRNA-21 / biotin-H2 / biotin-H1 / SA-ALP (curve blue). HCR, hybridization chain reaction; EIM, enzyme-induced metallization; MA, AuNPs-modified ITO microelectrode array; MBs, magnetic nanobeads; CP, capture probe; SA-ALP, streptavidin-alkaline phosphatase conjugate. Adapted from Ref. [42], Copyright (2019), with permission from Elsevier.

Figure 9. (A) Schematic diagram of the electrochemical miRNA biosensor based on enzyme-free signal amplification integrating rGO-PPy/AuNPs, CHA, and HCR. **(B)** Structures of H1, target, H2, H3, and H4, respectively. **(C)** DPVs for the detection of different concentrations of target microRNA with the proposed method. **(D)** The corresponding calibration plot obtained from the DPVs shown in (C). rGO, reduced graphene oxide; PPy, polypyrrole; AuNPs, gold nanoparticles; CHA, catalytic hairpin assembly; HCR, hybridization chain reaction. Adapted from Ref. [46], Copyright (2019), with permission from Elsevier.

Figure 10. Scheme for the electrochemical quantification of miRNA-21 through the target-driven CHA and ratiometric amplification strategy. Reprinted from Ref. [48], Copyright (2019), with permission from Elsevier.

Figure 11. (A) Schematic diagram of exosomal miRNA detection using a “sandwich” electrochemical exosomal miRNA sensor (SEEmiR). In the presence of target, electrode surface-assembled PNA probes specifically hybridize with SNA–miRNA complex. RuHex serves as an electroactive indicator by CC. (B) CVs (a) and CC curves (b) of the SEEmiR sensor assembled with PNA probe (gray line), after hybridization with miRNA in the absence (green line) and presence (orange line) of SNA after incubation with RuHex, respectively. ΔQ is the variation in the redox charge of RuHex before and after hybridization. (c) SWVs of PNA and DNA hybridization with miRNA-21 labeled with MB. From inset, PNA–miRNA shows a substantial signal enhancement over DNA–miRNA. (d) Optimization of assembly concentrations of PNA to obtain rational probe spacing at the interface and to maintain the maximal hybridization efficiency for SNA. (C) (a) CC curves of the SEEmiR sensor in response to different target miRNA-21 concentrations in the presence of SNA after incubation with RuHex. (b) ΔQ versus miRNA-21 concentrations. (c) CC curves of the SEEmiR sensor in response to different target miRNA-21 concentrations without SNA amplification. (d) Linear relationship between ΔQ and the logarithm of target miRNA-21 concentrations in the presence (orange line) and absence (blue line) of SNA amplification, respectively. (d) SNA renders the sensitivity improvement by 3 orders of magnitude (gray box). PNA, peptide nucleic acid; SNA, spherical nucleic acid; RuHex, $[\text{Ru}(\text{NH}_3)_6]^{3+}$; CC, chronocoulometry; MB, methylene blue. Adapted with permission from Ref. [51]. Copyright 2019 American Chemical Society. (2019) *Analytical Chemistry*, 91 (20), pp. 13198-13205

Figure 12. Schematic illustration of the ratiometric electrochemical biosensor for exosomal miRNA-21 detection. Reprinted from Ref. [56], Copyright (2020), with permission from Elsevier.

Figure 13. Schematic illustration of the preparation of the SH-RNA/MCH-AuNPs-SPCEs and the direct competitive hybridization assay developed for miRNA

quantification. Reprinted from Ref. [57], Copyright (2017), with permission from Elsevier.

Journal Pre-proof

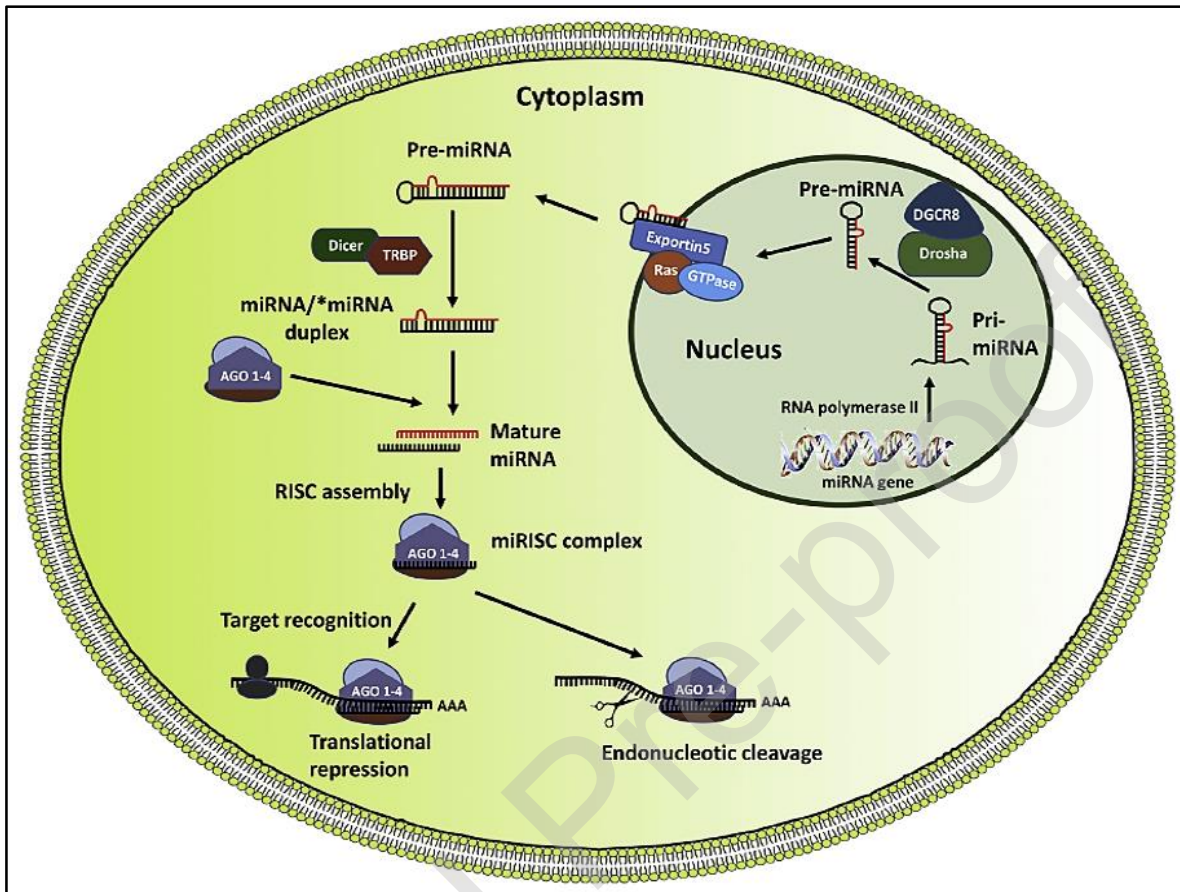


Figure 1. Nuclear and cytoplasmic processing of miRNAs and mechanisms of gene expression regulation. Reprinted from Ref. [4], Copyright (2020), with permission from Elsevier.

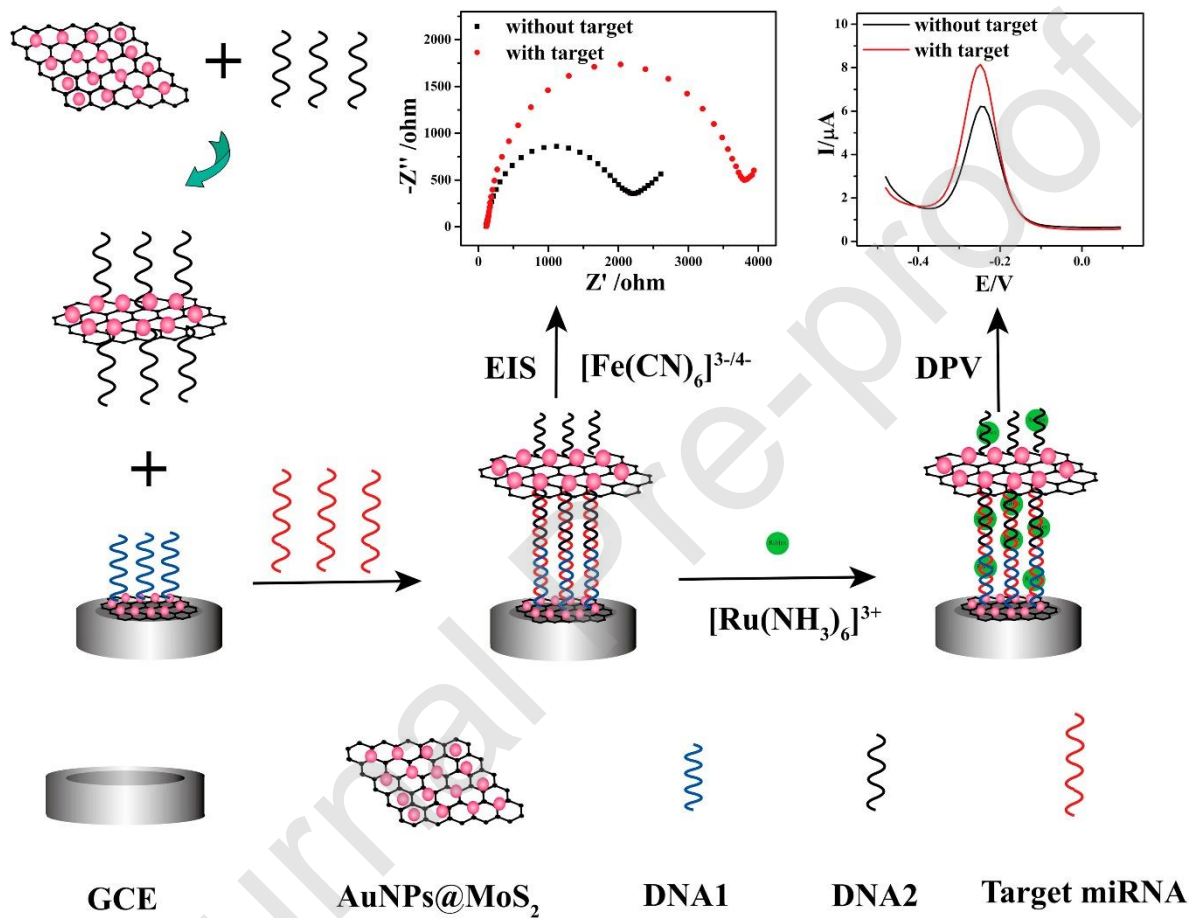


Figure 2. Schematic of label-free and dual mode electrochemical assay for miRNA-21 detection based on gold-nanoparticle-decorated MoS₂ nanosheet. Reprinted from Ref. [24], Copyright (2017), with permission from Elsevier.

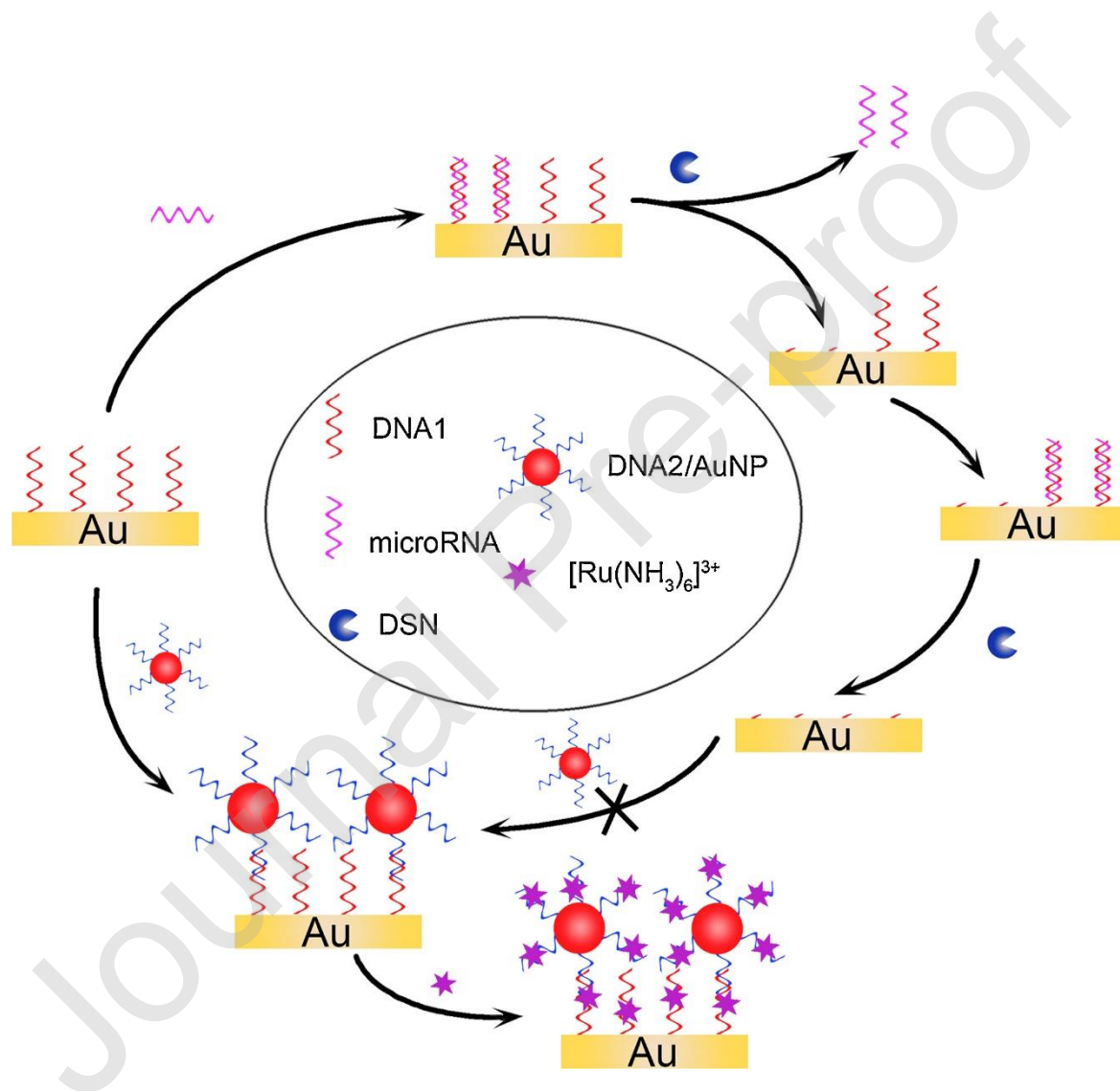


Figure 3. Scheme of the amplified detection of miRNA through the activity of DSN and the accumulation of the redox marker RuHex. Reprinted from Ref. [27], Copyright (2016), with permission from Elsevier.

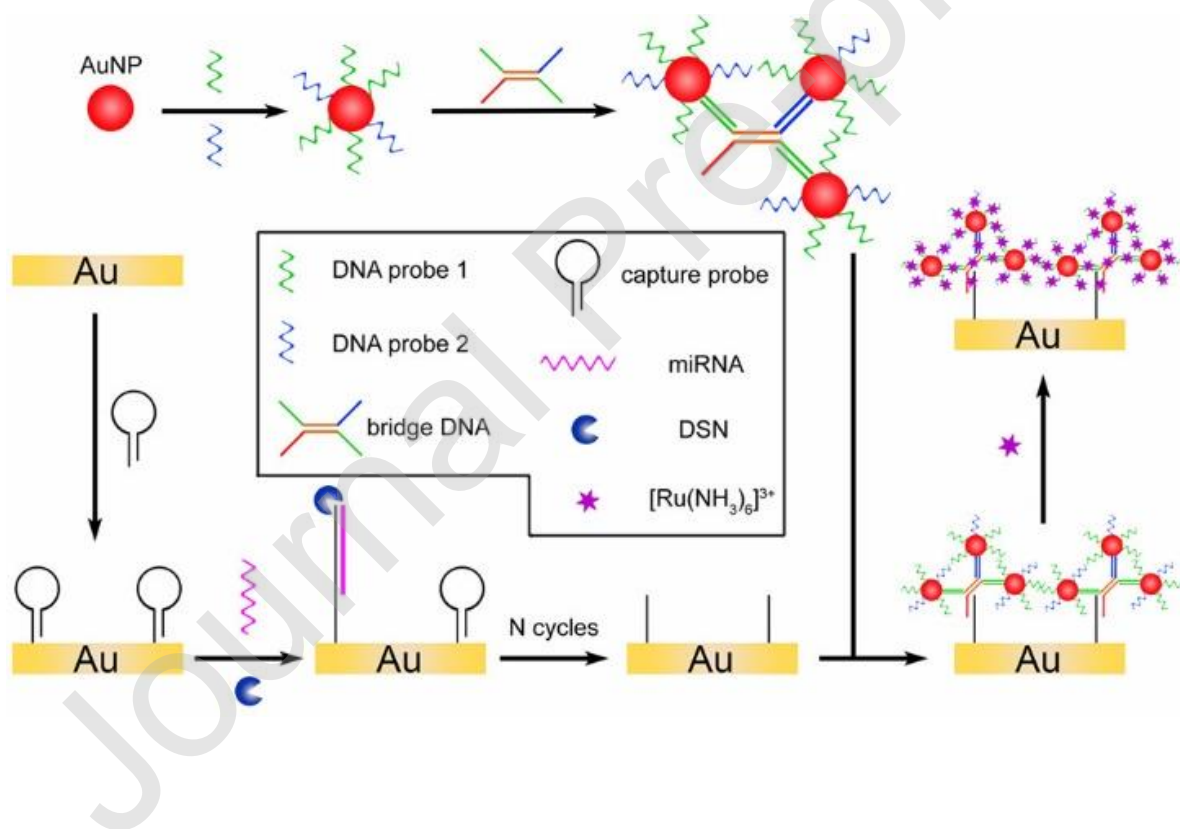


Figure 4. Scheme for the triple amplified detection of miRNA with electrochemical quantification through the accumulation of the redox marker RuHex. Reprinted from Ref. [28], Copyright (2020), American Chemical Society.

Journal Pre-proof

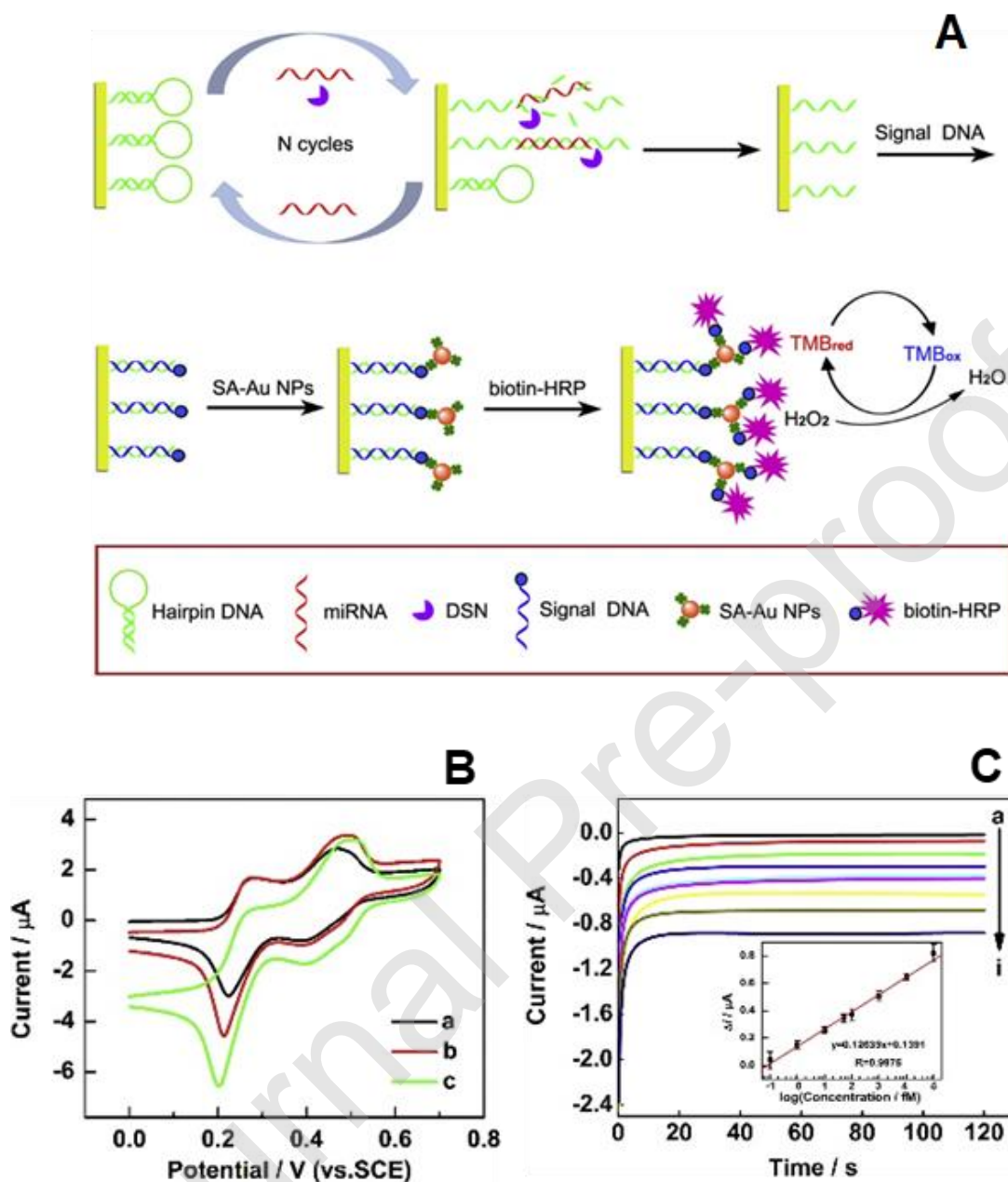


Figure 5. A) Scheme of the electrochemical miRNA biosensor based on DSN-assisted target recycling followed with AuNPs and HRP enzymatic signal amplification strategy. B) Cyclic voltammograms of the electrochemical biosensor monitoring the TMB redox reaction in the presence of: a) 0M, b) 100 fM, c) 100 pM miRNA-21. C) Chronoamperometric signals obtained for different concentrations of miRNA-21 a) to i) is 0.01fM, 1fM, 10 fM, 50 fM, 100 fM, 1 pM, 10 pM, 100, pM,

respectively. The inset is the linear calibration plot of Δi versus the logarithm of miRNA-21 concentration. Adapted from Ref. [30], Copyright (2019), with permission from Elsevier.

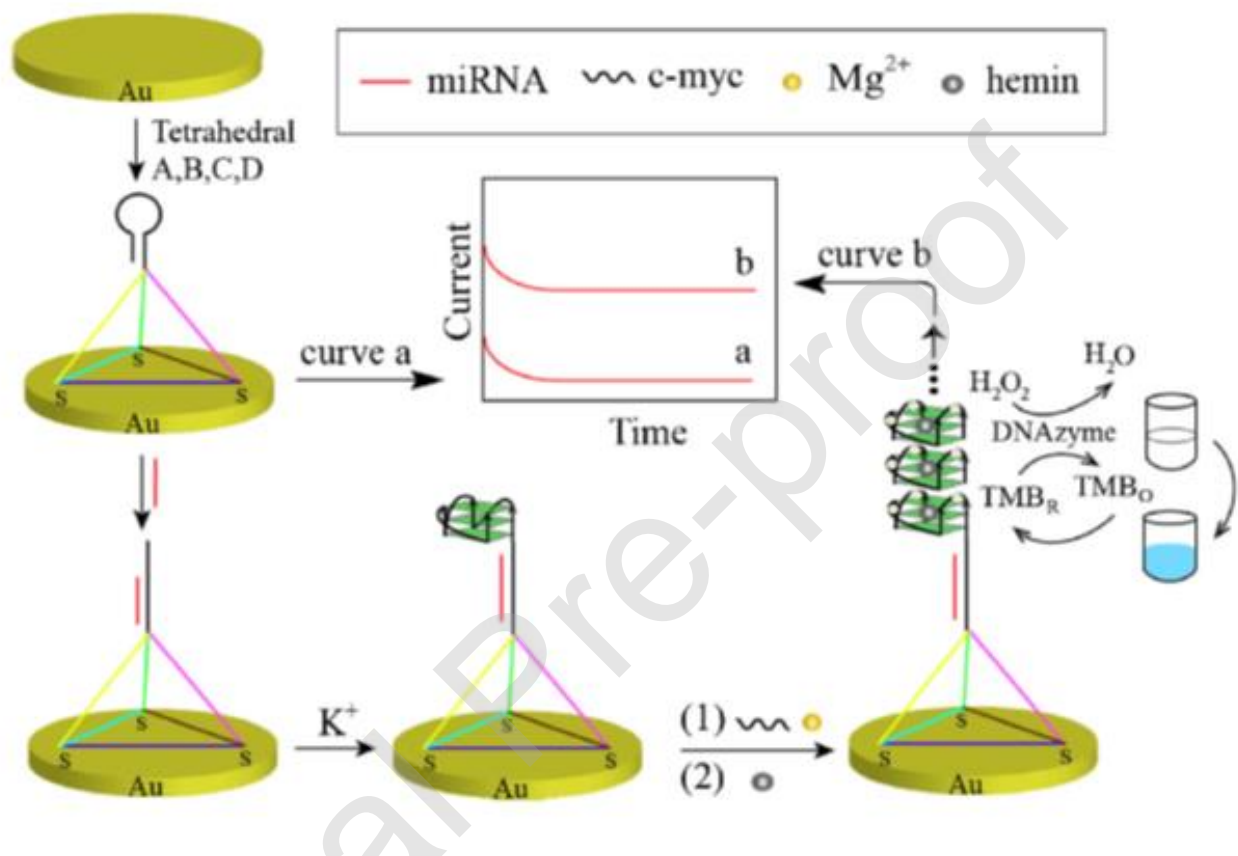


Figure 6. Schematic representation for the different steps during the building of the electrochemical miRNA biosensor and the electrochemical transduction. Adapted by permission from Springer Nature: Amperometric biosensor for microRNA based on the use of tetrahedral DNA nanostructure probes and guanine nanowire amplification, Huang, Y.L., Mo, S., Gao, Z.F., Chen, J.R., Lei, J.L., Luo, H.Q., Li, N.B., Copyright (2017)

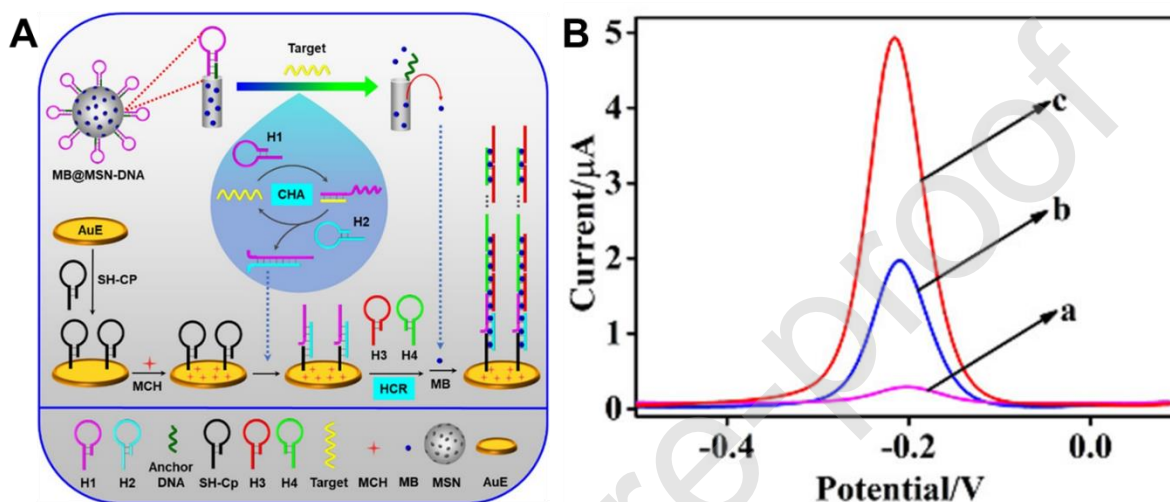


Figure 7. **(A)** Schematic diagram of MSNs and programmed CHA/HCR based electrochemical sensing platform for miRNA-21 ultrasensitive detection. **(B)** SWV response of the programmed CHA/HCR on SH-CP/MCH-modified AuE incubated with the mixtures of (a) MB@MSNs-DNA, H1, H2, and H4 probes, (b) target miRNA-21, MB@MSNs-DNA, and H2 probe, and (c) target miRNA-21, MB@MSNs-DNA, H2, H3, and H4 probes. MSNs, mesoporous silica containers; CHA, catalytic hairpin assembly; HCR, hybridization chain reaction; CP, capture probe; MCH, 6-mercaptohexanol; MB, methylene blue. Adapted with permission from Ref. [40]. Copyright 2019 American Chemical Society.

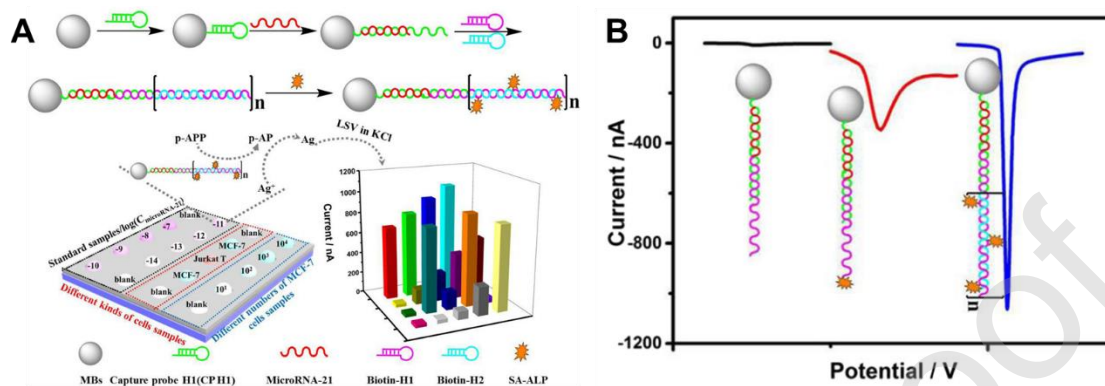


Figure 8. **(A)** Schematic diagram of the protocol for electrochemical detection of miRNA-21: capture of miRNA-21 and HCR (above), and EIM and electrochemical detection of multiple samples on the same MA (below). **(B)** LSVs under different conditions: MBs / CP H1 / miRNA-21 / biotin-H2 (curve black), MBs / CP H1 / miRNA-21 / biotin-H2 / SA-ALP (curve red), and MBs / CP H1 / miRNA-21 / biotin-H2 / biotin-H1 / SA-ALP (curve blue). HCR, hybridization chain reaction; EIM, enzyme-induced metallization; MA, AuNPs-modified ITO microelectrode array; MBs, magnetic nanobeads; CP, capture probe; SA-ALP, streptavidin-alkaline phosphatase conjugate. Adapted from Ref. [42], Copyright (2019), with permission from Elsevier.

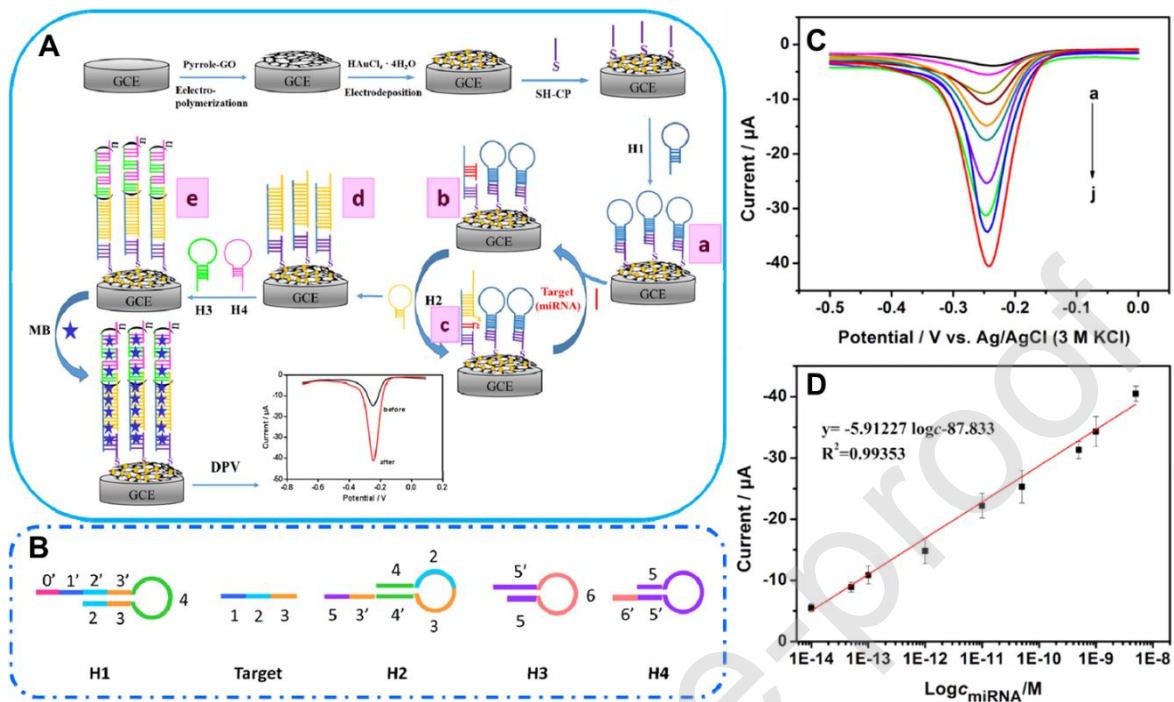


Figure 9. **(A)** Schematic diagram of the electrochemical miRNA biosensor based on enzyme-free signal amplification integrating rGO-PPy/AuNPs, CHA, and HCR. **(B)** Structures of H1, target, H2, H3, and H4, respectively. **(C)** DPVs for the detection of different concentrations of target microRNA with the proposed method. **(D)** The corresponding calibration plot obtained from the DPVs shown in (C). rGO, reduced graphene oxide; PPy, polypyrrole; AuNPs, gold nanoparticles; CHA, catalytic hairpin assembly; HCR, hybridization chain reaction. Adapted from Ref. [46], Copyright (2019), with permission from Elsevier.

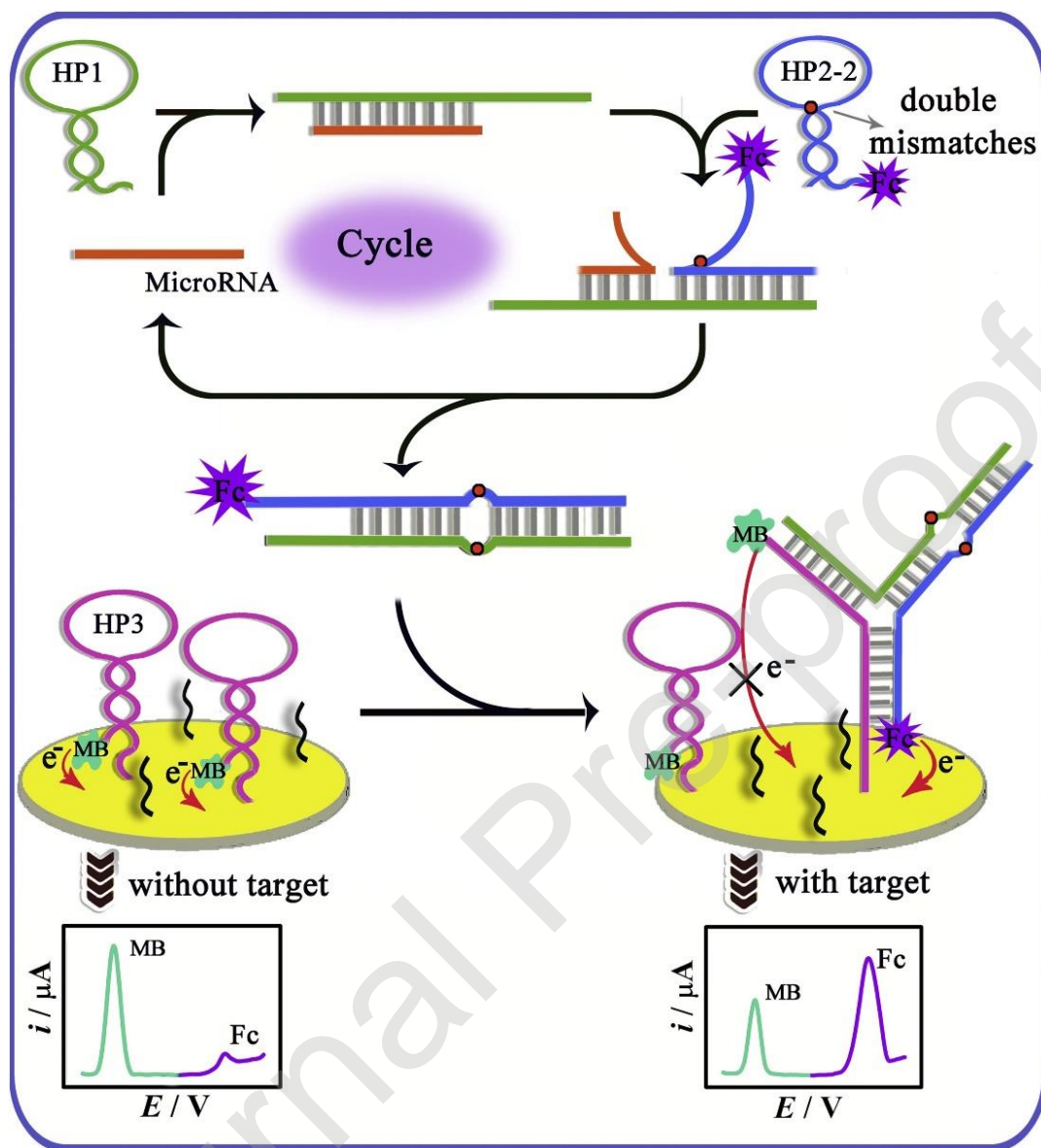


Figure 10. Scheme for the electrochemical quantification of miRNA-21 through the target-driven CHA and ratiometric amplification strategy. Reprinted from Ref. [48], Copyright (2019), with permission from Elsevier.

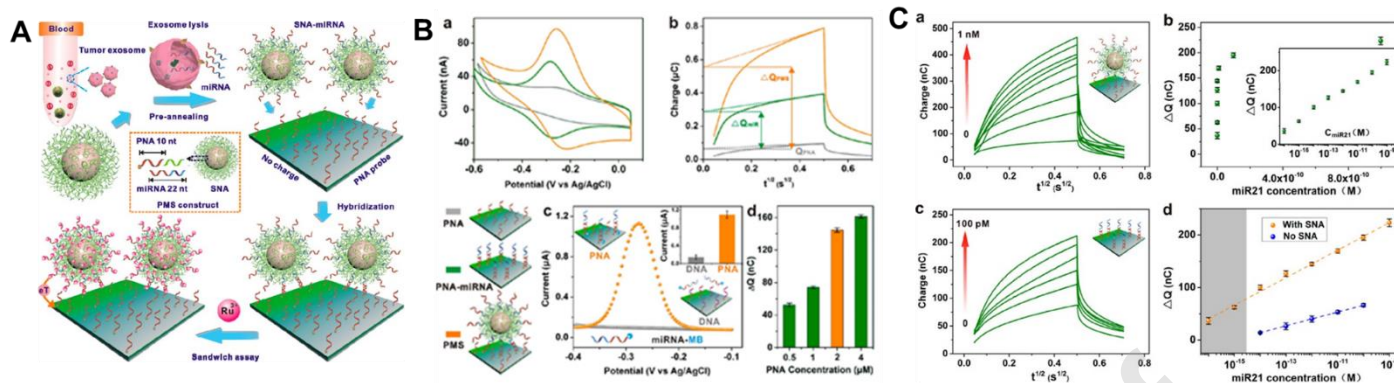


Figure 11. **(A)** Schematic diagram of exosomal miRNA detection using a “sandwich” electrochemical exosomal miRNA sensor (SEEmiR). In the presence of target, electrode surface-assembled PNA probes specifically hybridize with SNA–miRNA complex. RuHex serves as an electroactive indicator by CC. **(B)** CVs (a) and CC curves (b) of the SEEmiR sensor assembled with PNA probe (gray line), after hybridization with miRNA in the absence (green line) and presence (orange line) of SNA after incubation with RuHex, respectively. ΔQ is the variation in the redox charge of RuHex before and after hybridization. (c) SWVs of PNA and DNA hybridization with miRNA-21 labeled with MB. From inset, PNA–miRNA shows a substantial signal enhancement over DNA–miRNA. (d) Optimization of assembly concentrations of PNA to obtain rational probe spacing at the interface and to maintain the maximal hybridization efficiency for SNA. **(C)** (a) CC curves of the SEEmiR sensor in response to different target miRNA-21 concentrations in the presence of SNA after incubation with RuHex. (b) ΔQ versus miRNA-21 concentrations. (c) CC curves of the SEEmiR sensor in response to different target miRNA-21 concentrations without SNA amplification. (d) Linear relationship between ΔQ and the logarithm of target miRNA-21 concentrations in the presence (orange line) and absence (blue line) of SNA amplification, respectively. (d) SNA renders the sensitivity improvement by 3 orders of magnitude (gray box). PNA, peptide nucleic acid; SNA, spherical nucleic acid; RuHex, $[\text{Ru}(\text{NH}_3)_6]^{3+}$; CC, chronocoulometry; MB, methylene blue. Adapted with permission from Ref. [51]. Copyright 2019 American Chemical Society. (2019) Analytical Chemistry, 91 (20), pp. 13198-13205

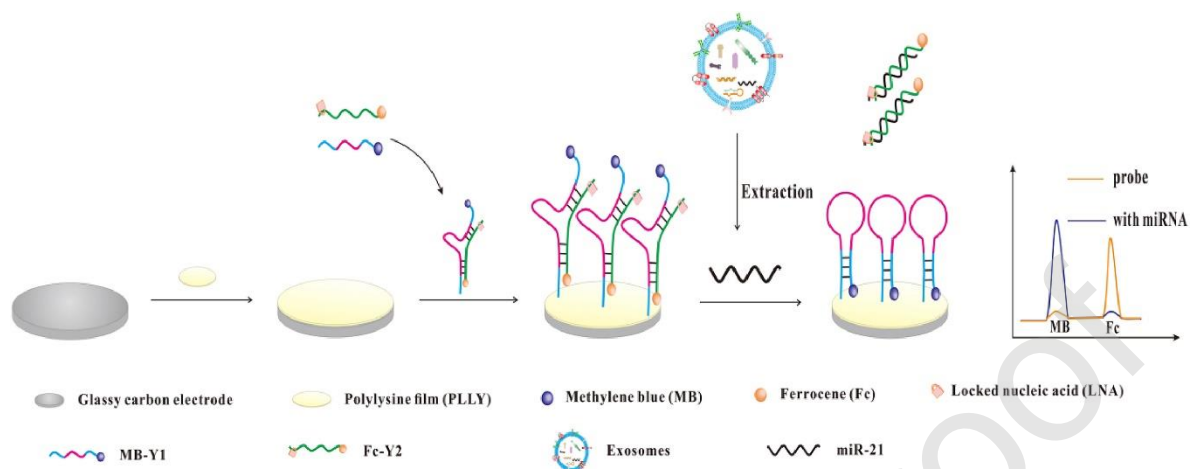


Figure 12. Schematic illustration of the ratiometric electrochemical biosensor for exosomal miRNA-21 detection. Reprinted from Ref. [56], Copyright (2020), with permission from Elsevier.

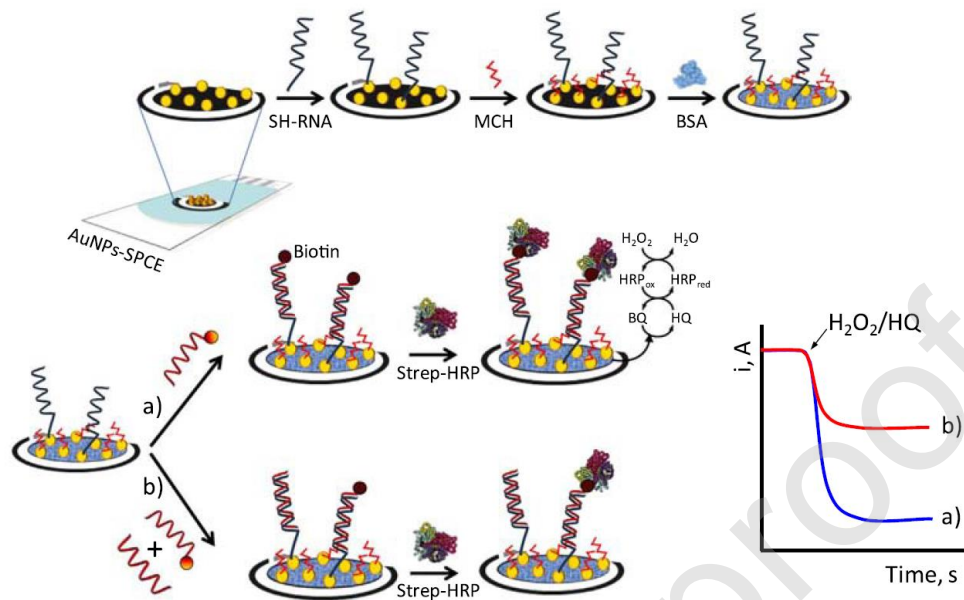


Figure 13. Schematic illustration of the preparation of the SH-RNA/MCH-AuNPs-SPCEs and the direct competitive hybridization assay developed for miRNA quantification. Reprinted from Ref. [57], Copyright (2017), with permission from Elsevier.

Table 1. Comparison of the analytical performance of the most relevant electrochemical miRNAs biosensors developed between 2017 and the beginning of 2020.

Non-amplified miRNAs electrochemical biosensors						
Target	Detection Method	Platform	LOD	LR	Real sample	Ref.
miRNA-21	DPV	GCE/PLLY/MB-DNA/LNA	2.3 fM	10 fM-70 fM	Exosomes samples	[56]
miRNA-21	Amperometry	SPCE/AuNPs/RNA-SH	25 fM	100 fM-25 pM	MCF-7 and MCF-10	[57]
miRNA-21	EIS DPV	PGE/PPy/DNA	12.25 nM 0.17 nM	-	MCF-7 and HUH-7 samples	[58]
miRNA-660	EIS	PGE/NrGO-CHIT/DNA	1.72 mg/mL	-	Fetal bovine serum samples	[59]
miRNA-21	SWV	ITO/PAA/AuNPs/DNA _p	1.0 fM	1.0 fM-100 pM	Human lung cancer cell (A549)	[60]
miRNA-21	DPV	FTO/CGO/Au-PtBNPs/SA/CP	1.0 fM	1.0 fM-1.0 μM	Human serum	[61]
miRNA-21	DPV	GCE/MoS ₂ @MB	68 fM,	0.1 pM-1.0 nM	Human serum	[62]
miRNA-122	DPV	Au/GO/PB	1.5 fM	10 fM-10 nM	Human serum	[63]
miRNA-21	SWV	GCE/AuNPs/Thi/MoS ₂	0.26 pM	1.0 pM-10 nM	Human serum	[64]
miRNA-103	SWV	GCE/AuNPs/SH-JUG-MHA/pDNA-103	100 fM	100 fM-5.0 nM	-	[65]
miRNA-21	DPV	AuNS/ssRNA/TB	78 aM	100 aM-1.0 nM	Human serum	[66]
miRNA-21	CV	Au/PPy/AgNF/PNA	10 fM	1.0 x 10 ⁻¹³ M-1.0 x 10 ⁻⁸ M	Human plasma	[67]
miRNA-375	SWV	SPE/SH-DNA	11.7 aM	10 aM-1.0 nM	Prostate cells	[68]

Amplification-based miRNAs electrochemical biosensors

Target	Detection Method	Signal Amplification Strategy	Electrode	LOD	LR	Real sample	Ref.
miRNA-21	Chronocoulometry	Graphene oxide-loaded iron oxide. Signal of [Ru(NH ₃) ₆] ³⁺ catalyzed by [Fe(CN) ₆] ³⁻	SPCE	1.0 fM	1.0 fM-1.0 nM	Ovarian cancer and non-cancerous cells	[22]
miR-107	Chronocoulometry	Gold-loaded nanoporous superparamagnetic iron oxide nanocubes (Au@NPFe ₂ O ₃ NC). Catalytic reduction of [Ru(NH ₃) ₆] ³⁺	SPCE	100 aM	100 aM-1.0 nM	Cancer tissues and non-cancerous tissues	[23]
miRNA-21	EIS DPV	AuNPs-decorated MoS ₂ nanosheet (AuNPs@MoS ₂) as electrode modifier and signal-amplifier element. Reduction current of [Ru(NH ₃) ₆] ³⁺ or charge transfer resistance of [Fe(CN) ₆] ^{3-/4-} .	GCE	7.08 fM 0.45 fM	10 fM-1.0 nM 1.0 fM-1.0 nM	Human serum	[24]
miRNA-21	Chronocoulometry	[Ru(NH ₃) ₆] ³⁺ accumulated at the hybrid between the capture thiolated-DNA immobilized at MoS ₂ nanosheets intimately coupled with electrodeposited AuNPs (AuNPs@MoS ₂)	SPE	100 aM	10 fM-10 pM	-	[25]
miR-29a-3p	Chronocoulometry	DSN-mediated hydrolysis of the DNA-1 strand at the (DNA-1/miRNA-29a-3p) surface heteroduplex, target release, decrease of the amount of (DNA-1/DNA-2-AuNPs) surface hybrid. Decrease of [Ru(NH ₃) ₆] ³⁺ electrostatically associated to this hybrid	Au	0.05 fM	0.1 fM-100 pM	Cells from healthy and infected patients with H1N1 influenza A virus	[27]
miRNA-21	Chronocoulometry	Triple signal amplification based on target-triggered cyclic DSN digestion and bridge DNA-AuNPs and preconcentration of [Ru(NH ₃) ₆] ³⁺ .	Au	6.8 aM	1.0 x 10 ⁻¹⁷ M-1.0 x 10 ⁻¹¹ M	Human serum	[28]
miRNA let-7d	SWV	Double-loop hairpin probe and doxorubicin-loaded AuNPs (AuNPs@Dox)	Au	0.17 pM	1.0 pM-10 nM	Human serum	[29]
miRNA-21	Amperometry	Hairpin DNA modified-gold electrode, DSN-assisted target recycling, and DNA/streptavidin-AuNPs to anchor the biotinylated HRP	Au	43 aM	0.1 fM-100 pM	A549 tumor cells	[30]
miRNA-21	DPV	MWCNTs@GONRs/AuNPs with DSN assisted target recycling and alkaline phosphatase-induced redox reactions	GCE	0.034 fM	1.0 x 10 ⁻¹⁶ M-1.0 x 10 ⁻¹⁰ M	Human serum	[31]

miRNA-21	SWV	Star-trigon structure and endonuclease mediated signal amplification using PDDA and AuNPs to anchor the MB labeled-capture probe.	GCE	30 aM	100 aM-1.0 nM	Human serum	[32]
miRNA-24	SWV	Cobalt oxide petals and poly(o-phenylenediamine) and covalent attachment of hyaluronic acid and methionine-gold nanoclusters as support of the “partial” probe/MB-reporter double strand.	GCE	33.3 fM	100 fM-0.1 μ M	Cancer cells	[33]
miRNA-141	DPV EIS	AuNPs and a hairpin-locked DNAzyme, generation of the “active” DNAzyme and successive activation cycles, and the fragments on the electrode surface capture produced numerous bioconjugates CuCo–CeO ₂ -signaling DNA.	GCE	33 aM	0.1 fM-10 nM	Human prostate-cancer and HeLa cells	[34]
miRNA-21	EIS	Neutravidin and a highly specific biotinylated DNA/LNA molecular beacon probe conjugated with AuNPs	GCE	0.3 pM	1.0 pM-1000 pM	Human serum	[35]
miRNA let-7a	DPV	Formation of trivalent DNAzyme junctions from the miRNA that initiated CHA of three hairpins into many trivalent DNAzyme junctions and subsequent generation of G-quadruplex	Au	0.46 fM	1.0 fM-1.0 nM	Human serum	[36]
miRNA-21	CV	MB mediated by Ir(III) complex intercalated at the surface generated G-quadruplex	Au	1.6 fM	5.0 fM-1.0 pM	Human serum	[37]
miRNA-21	Amperometry	Tetrahedral DNA nanostructures and G-quadruplex and hemin as a catalyst for TBM oxidation	Au	176 fM	500 fM-10 nM	Human serum	[38]
miRNA-21	DPV	Signal cascade amplification of DNA walkers	Au	67 aM	0.1 fM-100.0 fM	MCF-7 cells	[39]
miRNA-21	SWV	MB released from mesoporous silica nanospheres-hairpin H1, based on the enzyme-free amplification of CHA and HCR	Au	0.037 fM	0.1 fM-5.0 pM	Liver hepatocellular cells	[40]
miRNA-21	SWV	Phosphate backbone DNA strand and molybophosphate as redox probe	Au	0.5 fM	1.0 fM-1.0 nM	Human serum	[41]
miRNA-21	DPV	HCR and EIM, catalytic activity ALP	Au	0.84 fM	1.0 x 10 ⁻¹⁵ M-1.0 x 10 ⁻⁸ M	Human serum	[42]

miRNA-21	DPV	Hairpin capture probe immobilized at Fe ₃ O ₄ allowing HCR and the synergized catalytic reduction of hydrogen peroxide/TMB system in the presence of a Cu(II) planar complex	MGCE	33 aM	100 aM-100 nM	Human serum	[43]
miRNA-21	DPV	Cascade HCR as an enzyme-free isothermal with the intercalation of MB in the hyper-branched resulting dsDNA	Au	11 pM	30 pM-7.0 nM	Human serum	[44]
miRNA-141 miRNA-21	DPV	Fe ₃ O ₄ -NPs modified with thionine and ferrocene and target-triggered HCR	Au	0.44 fM 0.46 fM	1.0 fM-1.0 nM	Human breast cancer cells	[45]
miRNA-16	DPV	AuNPs/PPy-rGO, CHA and HCR	GCE	1.57 fM	10 fM-5.0 nM	Human serum	[46]
miRNA-21	EIS	ZrO ₂ -rGO-modified electrode coupled with CHA	GCE	4.3 x 10 ⁻¹⁵ M	1.0 x 10 ⁻¹⁴ M-1.0 x 10 ⁻¹⁰ M	MCF7 cells and human embryonic kidney cells	[47]
miRNA-21	SWV	Ratiometric scheme based on target driven CHA mismatched using three hairpins, H1, Fc-H2 with 2 mismatches and a thiolated-MB modified-H3	Au	1.1 fM	5.0 fM-0.1 nM	Cell extraction samples from MCF-7	[48]
miRNA-21	DPV	A conjugate ALP-Streptavidin and the detection from the naphthol oxidation signal in the presence of α -naphthyl phosphate	PGE	100 pM	200 pM-388 nM	-	[49]
miRNA-21	DPV	DNA-AuNPs, miRNA-21 and MWCNTs modified with a signaling DNA and labeled with thionine	GCE	0.032 pM	0.1 pM-12000 pM	-	[50]
miRNA-21	Chronocoulometry	A sandwich" electrochemical exosomal microRNA sensor using peptide nucleic acid as biorecognition element and spherical DNA as secondary probe	Au	49 aM	100 aM-1.0 nM	MCF-7 and HeLa cells	[51]
miRNA-21	DPV	Sandwich hybridization between thiolated-DNA probes at SPCE modified with GO-AuNPs nanohybrid and the signaling DNA conjugated with Fc-AuNPs-Streptavidin	SPCE	5 fM	10 fM-2.0 pM	Human serum	[52]
miRNA-21	DPV	RCA that produced a massive G-rich long ssDNAs to be used as matrix for the in situ synthesis of PdNPs	Au	8.6 aM	50 aM-100 fM	Human serum	[53]
miRNA-21	Amperometry	Anti DNA-RNA antibody anti DNA probe-miRNA heteroduplex and bacterial protein A (ProtA) conjugated	SPCE	0.4 pM	1.0 pM-100 pM	Cancer cells and tumor tissues	[54]

miRNA-155 miRNA-122	DPV	with HRP homopolymer (Poly-HRP40) as enzymatic label COF nanowire and melamine as platform for immobilizing the capture ssDNAs able to hybridize with the aptamers anti-miRNA155 and anti-miRNA-22 modified with shell-encoded AuNPs as signal labels	GCE	6.7 fM 1.5 fM	0.01 pM-1000 pM	Human serum	[55]
------------------------	-----	--	-----	------------------	-----------------	-------------	------

Target	Detection Method	Signal Amplification Strategy	Electrode	LOD	LR	Real sample	Ref.
miRNA-21	Chronocoulometry	Graphene oxide-loaded iron oxide. Signal of $[\text{Ru}(\text{NH}_3)_6]^{3+}$ catalyzed by $[\text{Fe}(\text{CN})_6]^{3-}$	SPCE	1.0 fM	1.0 fM-1.0 nM	Ovarian cancer and non-cancerous cells	[22]
miR-107	Chronocoulometry	Gold-loaded nanoporous superparamagnetic iron oxide nanocubes ($\text{Au}@ \text{NPF}_2\text{O}_3\text{NC}$). Catalytic reduction of $[\text{Ru}(\text{NH}_3)_6]^{3+}$	SPCE	100 aM	100 aM-1.0 nM	Cancer tissues and non-cancerous tissues	[23]
miRNA-21	EIS DPV	AuNPs-decorated MoS_2 nanosheet ($\text{AuNPs}@ \text{MoS}_2$) as electrode modifier and signal-amplifier element. Reduction current of $[\text{Ru}(\text{NH}_3)_6]^{3+}$ or charge transfer resistance of $[\text{Fe}(\text{CN})_6]^{3-/4-}$.	GCE	7.08 fM 0.45 fM	10 fM-1.0 nM 1.0 fM-1.0 nM	Human serum	[24]
miRNA-21	Chronocoulometry	$[\text{Ru}(\text{NH}_3)_6]^{3+}$ accumulated at the hybrid between the capture thiolated-DNA immobilized at MoS_2 nanosheets intimately coupled with electrodeposited AuNPs ($\text{AuNPs}@ \text{MoS}_2$)	SPE	100 aM	10 fM-10 pM	-	[25]
miR-29a-3p	Chronocoulometry	DSN-mediated hydrolysis of the DNA-1 strand at the (DNA-1/miRNA-29a-3p) surface heteroduplex, target release, decrease of the amount of (DNA-1/DNA-2-AuNPs) surface hybrid. Decrease of $[\text{Ru}(\text{NH}_3)_6]^{3+}$ electrostatically associated to this hybrid	Au	0.05 fM	0.1 fM-100 pM	Cells from healthy and infected patients with H1N1 influenza A virus	[27]
miRNA-21	Chronocoulometry	Triple signal amplification based on target-triggered cyclic DSN digestion and bridge DNA-AuNPs and preconcentration of $[\text{Ru}(\text{NH}_3)_6]^{3+}$.	Au	6.8 aM	$1.0 \times 10^{-17} \text{ M}$ - $1.0 \times 10^{-11} \text{ M}$	Human serum	[28]
miRNA let-7d	SWV	Double-loop hairpin probe and doxorubicin-loaded AuNPs ($\text{AuNPs}@ \text{Dox}$)	Au	0.17 pM	1.0 pM-10 nM	Human serum	[29]
miRNA-21	Amperometry	Hairpin DNA modified-gold electrode, DSN-assisted target recycling, and DNA/streptavidin-AuNPs to anchor the biotinylated HRP	Au	43 aM	0.1 fM-100 pM	A549 tumor cells	[30]
miRNA-21	DPV	MWCNTs@GONRs/AuNPs with DSN assisted target recycling and alkaline phosphatase-induced redox reactions	GCE	0.034 fM	$1.0 \times 10^{-16} \text{ M}$ - $1.0 \times 10^{-10} \text{ M}$	Human serum	[31]

miRNA-21	SWV	Star-trigon structure and endonuclease mediated signal amplification using PDDA and AuNPs to anchor the MB labeled-capture probe.	GCE	30 aM	100 aM-1.0 nM	Human serum	[32]
miRNA-24	SWV	Cobalt oxide petals and poly(o-phenylenediamine) and covalent attachment of hyaluronic acid and methionine-gold nanoclusters as support of the “partial” probe/MB-reporter double strand.	GCE	33.3 fM	100 fM-0.1 μ M	Cancer cells	[33]
miRNA-141	DPV EIS	AuNPs and a hairpin-locked DNAzyme, generation of the “active” DNAzyme and successive activation cycles, and the fragments on the electrode surface capture produced numerous bioconjugates CuCo–CeO ₂ -signaling DNA.	GCE	33 aM	0.1 fM-10 nM	Human prostate-cancer and HeLa cells	[34]
miRNA-21	EIS	Neutravidin and a highly specific biotinylated DNA/LNA molecular beacon probe conjugated with AuNPs	GCE	0.3 pM	1.0 pM-1000 pM	Human serum	[35]
miRNA let-7a	DPV	Formation of trivalent DNAzyme junctions from the miRNA that initiated CHA of three hairpins into many trivalent DNAzyme junctions and subsequent generation of G-quadruplex	Au	0.46 fM	1.0 fM-1.0 nM	Human serum	[36]
miRNA-21	CV	MB mediated by Ir(III) complex intercalated at the surface generated G-quadruplex	Au	1.6 fM	5.0 fM-1.0 pM	Human serum	[37]
miRNA-21	Amperometry	Tetrahedral DNA nanostructures and G-quadruplex and hemin as a catalyst for TBM oxidation	Au	176 fM	500 fM-10 nM	Human serum	[38]
miRNA-21	DPV	Signal cascade amplification of DNA walkers	Au	67 aM	0.1 fM-100.0 fM	MCF-7 cells	[39]
miRNA-21	SWV	MB released from mesoporous silica nanospheres-hairpin H1, based on the enzyme-free amplification of CHA and HCR	Au	0.037 fM	0.1 fM-5.0 pM	Liver hepatocellular cells	[40]
miRNA-21	SWV	Phosphate backbone DNA strand and molybophosphate as redox probe	Au	0.5 fM	1.0 fM-1.0 nM	Human serum	[41]
miRNA-21	DPV	HCR and EIM, catalytic activity ALP	Au	0.84 fM	1.0 x 10 ⁻¹⁵ M-1.0 x 10 ⁻⁸ M	Human serum	[42]

miRNA-21	DPV	Hairpin capture probe immobilized at Fe ₃ O ₄ allowing HCR and the synergized catalytic reduction of hydrogen peroxide/TMB system in the presence of a Cu(II) planar complex	MGCE	33 aM	100 aM-100 nM	Human serum	[43]
miRNA-21	DPV	Cascade HCR as an enzyme-free isothermal with the intercalation of MB in the hyper-branched resulting dsDNA	Au	11 pM	30 pM-7.0 nM	Human serum	[44]
miRNA-141 miRNA-21	DPV	Fe ₃ O ₄ -NPs modified with thionine and ferrocene and target-triggered HCR	Au	0.44 fM 0.46 fM	1.0 fM-1.0 nM	Human breast cancer cells	[45]
miRNA-16	DPV	AuNPs/PPy-rGO, CHA and HCR	GCE	1.57 fM	10 fM-5.0 nM	Human serum	[46]
miRNA-21	EIS	ZrO ₂ -rGO-modified electrode coupled with CHA	GCE	4.3 x 10 ⁻¹⁵ M	1.0 x 10 ⁻¹⁴ M-1.0 x 10 ⁻¹⁰ M	MCF7 cells and human embryonic kidney cells	[47]
miRNA-21	SWV	Ratiometric scheme based on target driven CHA mismatched using three hairpins, H1, Fc-H2 with 2 mismatches and a thiolated-MB modified-H3	Au	1.1 fM	5.0 fM-0.1 nM	Cell extraction samples from MCF-7	[48]
miRNA-21	DPV	A conjugate ALP-Streptavidin and the detection from the naphthol oxidation signal in the presence of α -naphthyl phosphate	PGE	100 pM	200 pM-388 nM	-	[49]
miRNA-21	DPV	DNA-AuNPs, miRNA-21 and MWCNTs modified with a signaling DNA and labeled with thionine	GCE	0.032 pM	0.1 pM-12000 pM	-	[50]
miRNA-21	Chronocoulometry	A sandwich" electrochemical exosomal microRNA sensor using peptide nucleic acid as biorecognition element and spherical DNA as secondary probe	Au	49 aM	100 aM-1.0 nM	MCF-7 and HeLa cells	[51]
miRNA-21	DPV	Sandwich hybridization between thiolated-DNA probes at SPCE modified with GO-AuNPs nanohybrid and the signaling DNA conjugated with Fc-AuNPs-Streptavidin	SPCE	5 fM	10 fM-2.0 pM	Human serum	[52]
miRNA-21	DPV	RCA that produced a massive G-rich long ssDNAs to be used as matrix for the in situ synthesis of PdNPs	Au	8.6 aM	50 aM-100 fM	Human serum	[53]
miRNA-21	Amperometry	Anti DNA-RNA antibody anti DNA probe-miRNA heteroduplex and bacterial protein A (ProtA) conjugated	SPCE	0.4 pM	1.0 pM-100 pM	Cancer cells and tumor tissues	[54]

		with HRP homopolymer (Poly-HRP40) as enzymatic label					
miRNA-155	DPV	COF nanowire and melamine as platform for immobilizing the capture ssDNAs able to hybridize with the aptamers anti-miRNA155 and anti-miRNA-22 modified with shell-encoded AuNPs as signal labels	GCE	6.7 fM 1.5 fM	0.01 pM-1000 pM	Human serum	[55]
miRNA-122							

LOD: limit of detection; LR: linear range; SPCE: screen-printed carbon electrode; EIS: electrochemical impedance spectroscopy; DPV: differential pulse voltammetry; AuNPs: gold nanoparticles; GCE: glassy carbon electrode; DNA: deoxyribonucleic acid; SPE: screen-printed electrode; DSN: duplex specific nuclease; SWV: square wave voltammetry; HRP: horseradish peroxidase; MWCNTs@GONRs: multi-walled carbon nanotubes@graphene oxide nanoribbons; PDDA: poly(diallyldimethylammonium) chloride; MB: methylene blue; LNA: locked nucleic acid; CHA: catalytic hairpin assembly; CV: cyclic voltammetry; TBM: 3,3',5,5'-tetramethylbenzidine; HCR: hybridization chain reaction; EIM: enzyme-induced metallization; ASV: anodic stripping voltammetry; MGCE: magnetic glassy carbon electrode; Fe₃O₄-NPs: magnetite nanoparticles; Au/PPy-rGO: polypyrrole-reduced graphene oxide; rGO: reduced graphene oxide; MCF7: human breast cancer cell lines; PdNPs: palladium nanoparticles; AgNC: silver nanocluster; ALP: alkaline phosphatase; PGE: pencil graphite electrode; MWCNTs: multi-walled carbon nanotubes; GO: graphene oxide; Fc: ferrocene; RCA: rolling circle amplification; ssDNA: single-stranded DNA; COF: covalent-organic framework.

LOD: limit of detection; LR: linear range; DPV: differential pulse voltammetry; GCE: glassy carbon electrode; PLY: polylysine; MB-DNA: methylene blue-modified DNA probe; LNA: locked nucleic acid; SPCE: screen-printed carbon electrode; AuNPs: gold nanoparticles; MCF-7: human breast cancer cell lines; MCF-10: non-tumorigenic epithelial breast cell line; EIS: electrochemical impedance spectroscopy; PGE: pencil graphite electrode; PPy: polypyrrole; HUH-7: human liver cell line; NrGO-CHIT: nitrogen doped reduced graphene oxide-chitosan; SWV: square wave voltammetry; ITO: indium tin oxide; PAA: poly(acrylic acid); RuHex: hexaammineruthenium(III) chloride; FTO: fluorine tin oxide; CGO: carboxylated graphene oxide; Au-PtBNPs: Au-Pt bimetallic nanoparticles; SA: streptavidin; CP: capture probe; GO: graphene oxide; PB: prussian blue; Thi: thionine; SH-JUG: 5-hydroxy-3-hexanedithiol-1,4-naphthoquinone; MHA: 6-mercaptohexanoic acid; AuNS: gold nanoparticles superlattices; ssRNA: single-stranded RNA; TB: toluidine blue; AgNF: silver nanofoam; PNA: peptide nucleic acid; SPE: screen-printed electrode.

TABLE 1. Comparison of the analytical performance of the most relevant electrochemical miRNAs biosensors developed between 2017 and the beginning of 2020.